พารามิเตอร์ที่มีผลต่อสัณฐานวิทยาและโครงสร้างเคมีของคาร์บอนแบล็กที่สังเคราะห์ด้วยกระบวนการแอเซทิลีนแบล็ก

นางสาวพิมพ์ชนก เลาห์ทวีรุ่งเรือง

วิทยานิพนธ์นี้เป็นส่วนหนึ่งของการศึกษาตามหลักสูตรปริญญาวิทยาศาสตรมหาบัณฑิต
สาขาวิชาปิโตรเคมีและวิทยาศาสตร์พอลิเมอร์
คณะวิทยาศาสตร์ จุฬาลงกรณ์มหาวิทยาลัย
ปีการศึกษา 2559

PARAMETERS AFFECTING MORPHOLOGY AND CHEMICAL STRUCTURE OF CARBON BLACK SYNTHESIZED BY ACETYLENE BLACK PROCESS

Miss Pimchanok Laowtaweerungruang

A Thesis Submitted in Partial Fulfillment of the Requirements
for the Degree of Master of Science Program in Petrochemistry and Polymer Science
Faculty of Science
Chulalongkorn University
Academic Year 2016

Thesis Title	PARAMETERS AFFECTING MORPHOLOGY AND CHEMICAL STRUCTURE OF CARBON BLACK SYNTHESIZED BY ACETYLENE BLACK PROCESS
By	Miss Pimchanok Laowtaweerungruang
Field of Study	Petrochemistry and Polymer Science
Thesis Advisor	Prompong Pienpinijtham, Ph.D.

Accepted by the Faculty of Science, Chulalongkorn University in Partial Fulfillment of the Requirements for the Master's Degree

.....Dean of the Faculty of Science
(Associate Professor Polkit Sangvanich, Ph.D.)

THESIS COMMITTEE

.....Chairman
(Professor Pattarapan Prasassarakich, Ph.D.)

.....Thesis Advisor
(Prompong Pienpinijtham, Ph.D.)

.....Examiner
(Chatr Panithipongwut Kowalski, Ph.D.)

.....External Examiner
(Nattawadee Wisitruangsakul, Ph.D.)

พิมพ์ชนก เลาห์ทวีรุ่งเรือง : พารามิเตอร์ที่มีผลต่อสัณฐานวิทยาและโครงสร้างเคมีของคาร์บอนแบล็กที่สังเคราะห์ด้วยกระบวนการแอเซทิลีนแบล็ก (PARAMETERS AFFECTING MORPHOLOGY AND CHEMICAL STRUCTURE OF CARBON BLACK SYNTHESIZED BY ACETYLENE BLACK PROCESS) อ.ที่ปรึกษาวิทยานิพนธ์หลัก: อ. ดร. พร้อมพงศ์ เพียรพินิจธรรม , 70 หน้า.

แอเซทิลีนแบล็กเป็นวัสดุที่ถูกนำมาใช้เป็นองค์ประกอบในงานทางด้านต่าง ๆ อย่างแพร่หลาย เช่น อุปกรณ์อิเล็กทรอนิก วัสดุสำหรับขั้วอิเล็กโทรด สี สารประกอบสำหรับพอลิเมอร์และวัสดุรองรับตัวเร่งปฏิกิริยา นอกจากสมบัติทางไฟฟ้าของแอเซทิลีนแบล็ก สมบัติอื่น ๆ ก็มีความสำคัญสำหรับการนำไปประยุกต์ใช้ในรูปแบบที่หลากหลายด้วย เนื่องจากสมบัติของแอเซทิลีนแบล็กขึ้นอยู่กับสัณฐานวิทยาและโครงสร้างทางเคมีซึ่งสามารถควบคุมได้ด้วยพารามิเตอร์ที่ใช้ในการสังเคราะห์ หรือการปรับปรุงสมบัติก่อนและหลังการสังเคราะห์ ในงานวิจัยนี้ ผู้วิจัยได้ทำการศึกษา ผลของอุณหภูมิ ความเข้มข้นของแอเซทิลีน และระยะเวลาที่สารอยู่ภายในเตาปฏิกรณ์ที่มีต่อสัณฐานวิทยา และโครงสร้างทางเคมีของแอเซทิลีนแบล็กที่สังเคราะห์ ผ่านกระบวนการสลายตัวด้วยความร้อน จากผลการทดลองพบว่า ที่ช่วงเริ่มต้น พลังงานความร้อนจะช่วยเร่งอัตราเร็วในการเกิดนิวเคลียสที่เป็นปัจจัยสำคัญในการเกิดอนุภาคขนาดเล็กทั้งในเชิงของอนุภาคเดี่ยวและอนุภาคกลุ่ม และยังช่วยผลักดันการเกิดปฏิกิริยาตลอดระยะเวลาที่มีการให้พลังงานความร้อน ในสภาวะที่อุณหภูมิสูงจะผลักดันให้เกิดการเชื่อมติดระหว่างขอบของผลึกที่มีลักษณะคล้ายแกรไฟต์ (L_a) พร้อมกับการหายไปของหมู่ฟังก์ชันของสารอินทรีย์ ซึ่งหมู่ฟังก์ชันเหล่านั้นหมดไปหลังจากที่เพิ่มอุณหภูมิสูงขึ้นมากกว่า 1100 องศาเซลเซียส ในส่วนของความเข้มข้นแอเซทิลีน พบว่าเมื่อความเข้มข้นของสารตั้งต้นสูงขึ้น ระบบจะอิ่มตัวมากขึ้นและผลักดันให้เกิดการชนกันระว่างโมเลกุลและอนุภาค และทำให้เกิดนิวเคลียสมากขึ้นเช่นเดียวกันกับอิทธิพลของอุณหภูมิ การชนกันของอนุภาคส่งเสริมให้เกิดขนาดของอนุภาคกลุ่มที่ใหญ่ขึ้น สำหรับผลของระยะเวลาที่สารอยู่ภายในเตาปฏิกรณ์ ระยะเวลาที่ยาวนานขึ้นจะช่วยขยายระยะเวลาในการโตของอนุภาคคาร์บอนทำให้ไปเพิ่มขนาดของอนุภาคเดี่ยว และอนุภาคกลุ่ม รวมไปถึงขนาดของ L_a จากผลการทดลอง อุณหภูมิที่ใช้ในการสังเคราะห์เป็นพารามิเตอร์สำคัญในการเกิดแอเซทิลีนแบล็ก ในขณะที่ความเข้มข้นของแอเซทิลีนและระยะเวลาที่สารอยู่ภายในเตาปฏิกรณ์ส่งผลเพียงเล็กน้อยต่อโครงสร้างของแอเซทิลีนแบล็ก

สาขาวิชา ปิโตรเคมีและวิทยาศาสตร์พอลิเมอร์ ลายมือชื่อนิสิต .....

ปีการศึกษา 2559 ลายมือชื่อ อ.ที่ปรึกษาหลัก .....

5772081723 : MAJOR PETROCHEMISTRY AND POLYMER SCIENCE

KEYWORDS: ACETYLENE BLACK / CARBON BLACK / ACETYLENE

PIMCHANOK LAOWTAWEERUNGRUANG: PARAMETERS AFFECTING MORPHOLOGY AND CHEMICAL STRUCTURE OF CARBON BLACK SYNTHESIZED BY ACETYLENE BLACK PROCESS. ADVISOR: PROMPONG PIENPINIJTHAM, Ph.D., 70 pp.

Acetylene black is widely used as a composite in various applications such as electronic devices, electrode materials, pigments, polymer composites, and catalyst supports. Not only its unique property of electrical conductivity but also other properties are required for various applications. The properties of acetylene black mostly depend on its morphological and chemical structures which can be controlled by synthesis parameters or modified by pre- and post-treatment. In this work, we observe the effect of temperature, acetylene concentration, and residence time on morphological and chemical structures of synthesized acetylene black through thermal decomposition process. The results show that, at an initial state, heat energy accelerates the nucleation rate, which provides smaller particles in both of primary and aggregate forms, and induces the reaction over the heated area. Higher temperature condition contributes to the sintering between crystal edges (L_a) and to the elimination of organic functional groups which totally disappear over 1100 °C. Higher concentration of feedstock generates higher saturated system which drives the collision between molecules and particles. It also induces the nucleation as the effect of temperature. Then, active collisions of particles push the larger size of aggregate structure. The long residence time also expands the growth period of carbon particles which increases the sizes of primary particles, aggregates, and L_a. In addition, synthesis temperature acts as a key parameter in the formation of acetylene black. The acetylene concentration and residence time slightly affect the acetylene black structure.

Field of Study: Petrochemistry and Polymer Science

Academic Year: 2016

Student's Signature .....

Advisor's Signature .....

ACKNOWLEDGEMENTS

Firstly, I would like to thank my parents for all their supports, continuous encouragement, understanding my decision, and spending the time together over the time of my life.

I would like to express my sincere gratitude to my adviser Dr. Prompong Pienpinijtham who helped me fulfilled myself through learning in both wrong and right ways, efforted to understand my thinking ways, helped me in all the time of research and writing thesis, tried to explain the theoretical information and other knowledge in simple ways, and enlightened me on the gloomy sides when I needed along my master study and research from beginning to the end.

I would like to thank all of my relatives and friends who willingly shared the moment and their cheerfulness with me, and their endlessly supported.

I would like to thank for the cute character of SRU members and my decision which brought me to access in this research unit. Thank you SRU members for their friendliness, kindness, comfortable atmosphere over the time of studying and doing all the activities. Their sufficient research facilities (Scientific instruments) help me achieved my efficiency results on the research project. Group meeting, all members sharing their knowledge, which helped me point out my mistakes.

I would like to express my gratitude to all research fund from IRPC Public Company Limited and Chulalongkorn university. Furthermore, I would like to thank all the encouragement, knowledge, and morality from studying at Chulalongkorn university.

Finally, I would like to thank my patience on the master research life that gave me the good training in many aspects.

CONTENTS

Page

Page

LIST OF TABLES

LIST OF FIGURES

LIST OF ABBREVIATIONS AND SYMBOLS

SEM	: scanning electron microscope
SEI	: secondary electron imaging
DLS	: dynamic light scattering
FT-IR	: Fourier-transform infrared
IR	: infrared
Ge IRE	: germanium internal reflection element
XRD	: X-ray diffraction
DLS	: dynamic light scattering
HRTEM	: high-resolution transmission electron microscope
BET	: Brunauer-Emmett-Teller
ATR	: attenuated total reflection
MCT	: mercury-cadmium-tellurium
HACA	: hydrogen-abstraction and carbon-addition
SWCNT	: single wall carbon nanotube
PVP	: polyvinylpyrrolidone
PAHs	: polycyclic aromatic hydrocarbons
LPAHs	: large polycyclic aromatic hydrocarbons
SPAHs	: small polycyclic aromatic hydrocarbons
DI	: de-ionized
STP	: standard conditions for gases
IUPAC	: international union of pure and applied chemistry
ID	: internal diameter
Eq.	: equation
FWHM or B	: full width at half maxima
K	: constant value
D	: disorder
G	: graphitic
d	: interplana spacing

n	: reflection order
I	: intensity
p	: pressure
V	: volume
E_L	: laser energy
λ	: wavelength
α	: alpha
θ	: theta
π	: pi
L_c	: length in c-axis of graphite crystal (crystal height)
L_a	: length in a-axis of graphite crystal (in plane)
L_D	: distance between defect
h	: hour
min	: minute
s	: second
g	: gram
mg	: milligram
cm	: centimeter
mm	: millimeter
μm	: micrometer
nm	: nanometer
cm^{-1}	: reciprocal centimeter
m^2	: square centimeter
cm^3	: cubic centimeter
L	: liter
mL	: milliter
kV	: kilovolt
eV	: electron volt
mW	: milliwatt
mA	: milliampere

%wt	: weight by weight percent
%v/v	: volume by volume percent
%w/v	: weight by volume percent
deg, °	: degree
° C	: degree celsius

CHAPTER I

INTRODUCTION

Carbon black is a material which is initially generated by incomplete combustion of organic material. The smallest unit in its structure is a micro-aggregate structure which composes of several nano-spherical particles. It has excellent properties due to different arrangements of microstructure and chemical forms inside the particle. In present, carbon black has been utilized in various applications such as polymer additives, pigments, and electronic devices, *etc.* due to its morphological and chemical structures which affect color tone, specific surface area, particle size, purity of carbon content, and crystallinity. Nowadays, the major consumer of carbon black is a rubber industry. Protocols of carbon black synthesis have been continuously developed. Numerous protocols of carbon black synthesis including lamp black, thermal black, gas black, furnace black, and acetylene black are shown in Table 1.1.

Table 1.1 Protocols of carbon black synthesis [1]. Copyright 1993 MARCEL DEKKER, INC.

Process	Precursors	Reaction	Collecting procedures	Carbon black features
Lamp black (First process)	oil or other raw materials	incomplete combustion on metallic plate	trapping by cooling metal plate	oxidized carbon black, broad particle size distribution, and low yield
Channel black	natural gas	incomplete combustion	impingement	oxidized carbon black and low yield
Gas black	vaporized oil	incomplete combustion	impingement	oxidized carbon black and low yield
Thermal black	oil or petroleum gas	thermal decomposition (batch)	bag filter	non-oxidized carbon black and large particle size
Furnace black (General procedure)	oil or petroleum gas	incomplete combustion	water quenching and bag filter	various grade of black
Acetylene black	acetylene gas	thermal decomposition	bag filter	non-oxidized carbon black, small particle size, high surface area, and high crystallinity

From Table 1. 1, the syntheses of carbon black use various types of feedstock to generate carbon black such as oil, natural gas, acetylene, *etc*. The different protocols for synthesizing carbon black give differences in a morphological structure (particle size, structure complication, surface area, *etc.*) and a chemical structure (type and distribution of chemical functional groups). However, acetylene black synthesis is a specific protocol generating a large size of crystal structures (L_a), which is led to be a high electrical property, because a precursor (acetylene) contains π-bond itself.

Acetylene is a by-product gas from petrochemical separation and stream cracking process which generates a main product of olefin being a main industry. Hence, petrochemical industry attempts to develop a proper manufacture to increase a value of acetylene by turning acetylene to acetylene black (carbon black).

Since each application requires specific morphological and chemical structure of acetylene black, the process for producing acetylene black has been evolved and developed, as shown on Table 1.2.

Table 1.2 Literature reviews of acetylene black

Authors/Year	Precursors	Protocol	Studying parameters	Application	Results
M. J .Katz /1956 [2]	Acetylene black	Graphitization	Temperature	-	Effect of temperature on surface properties
C. Giet /1981 [3]	Acetylene	Incomplete combustion	-	Electric cells	High electrical conductivity and high absorptive power
H.K.Orban /1963 [4]	Benzene and aromatic oil	Electric arc	1. Stabilizer gas 2. Feed	Rubber oil absorption	High structure carbon black
K .S. Bolouri /1986 [5]	Methane	Plasma process with argon	1. Flow rate 2. Temperature (plasma power) 3. Rate of cooling	Replacing that time expensive method	High quality of acetylene black low energy efficiency
Mendiara / 2005 [6]	Acetylene	Incomplete combustion	1. Flow rate 2. Concentration 3. Oxidizing agent 4. Water	Engine	Effect of process parameter on carbon conversion
K. Ono /2013 [7]	Benzene and acetylene	Thermal decomposition	1. Concentration 2. Temperature	Electric cells	Effect of process parameter on aggregate shape and primary particle diameter

A lot of researchers study about the synthesis of acetylene black in order to improve properties of acetylene black. Acetylene black is studied through basic one-step synthesis using different precursors and protocols or multi-step synthesis using additional processes in periods of time before and after synthesis (pre-heated feedstock and heat treatment of product). All processes are studied to meet the expected properties and to fulfill desired materials. Nevertheless, key parameters affecting acetylene black process still need further explanation.

In this work, we focus on mechanism of acetylene black synthesis method and study on main synthesizes parameters to know how the important parameters control the morphological and chemical structures of synthesized acetylene black carried out in the thermal decomposition reaction of a precursor as acetylene. The synthesized acetylene black characters are investigated using various techniques: scanning electron microscope (SEM) and dynamic light scattering (DLS), nitrogen adsorption-desorption analyzer in order to study the morphology and DXR Raman microscope, Fourier-transform infrared spectrometer (FT-IR) and X-ray powder diffractometer (XRD) in order to study the chemical structure. The results of this work can be used to develop reactor and control the expected characteristic features of acetylene black which fulfill the need on each application.

1.1 The objectives

Studying parameters which affect the morphology and chemical structures of carbon black synthesized by acetylene black process to get the expected characteristic features allowing each application.

1.2 Scopes of research

Studying the processing parameters which affect on acetylene black synthesis through the thermal decomposition reaction of acetylene with various synthesis temperatures, acetylene concentrations, and residence times using various characterization techniques to investigate their characteristic features.

CHAPTER II

THEORETICAL BACKGROUND

2.1 Carbon

Carbon is a highly essential substance which is widely used for serving in various applications such as electronics, reinforcement, sensors, pigments, and adsorbents due to their suitable properties of carbon forms. Different bondings of each carbon structure, such as graphene, fullerene, graphite, carbon dot, coal, carbon black, and others, drive onward the plenty of functions. Allotropes of carbon are carbon-carbon materials which have different structures. One aspect of the differences is sp, sp^2 and sp^3 hybridizations creating the different structures of solid elemental carbon. Another aspect of the differences is physical structure (morphology). Their forms can be amorphous, crystal, or mixture of them. Fig. 2.1 summarizes the solid carbon structure in hybridization, stereochemistry, and relative structure.

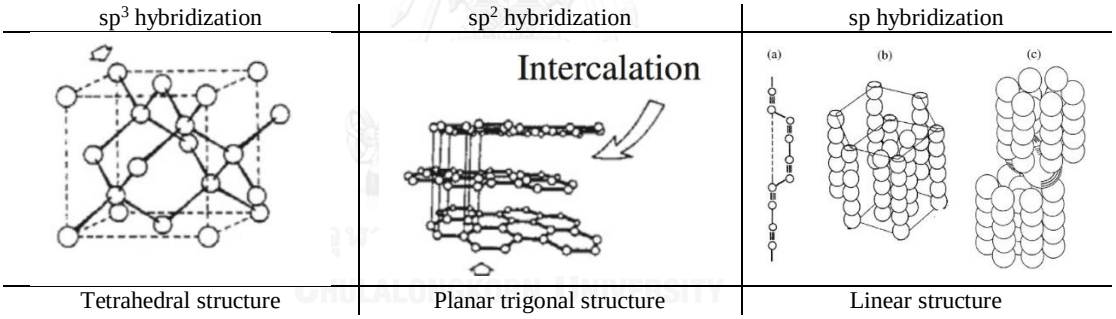

Fig. 2.1 Solid carbon structure stereochemistry and relative structures [8].
Copyright 2014 Tsinghua University Press Limited, Elsevier Inc.

There are allotropes of carbon which differ in degrees of structural or mixing ratio of molecular structure, such as carbon nanotube, fullerene (C_{60}), coal, carbon black, soot, pristine, *etc.*, being different in their properties. Structure of carbon allotropes are shown in Fig. 2.2.

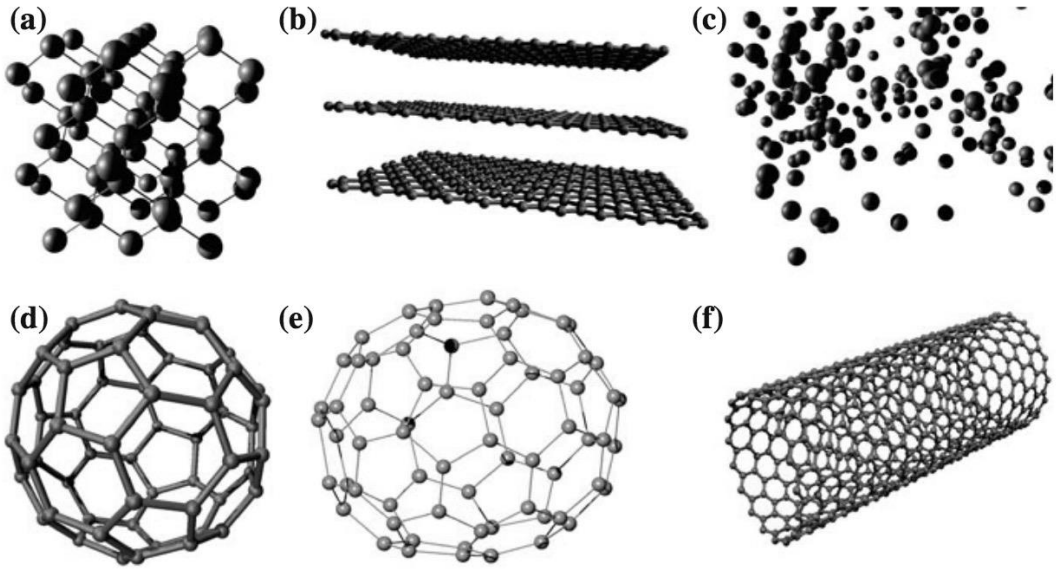

Fig. 2.2 Allotropes of carbon (a) diamond (b) graphite (c) amorphous carbon (d) fullerene C_{60} (e) Ellipsoidal fullerene C_{70} (f) single wall carbon nanotube (SWCNT) [9]. Copyright 2012 Springer-Verlag Berlin Heidelberg.

2.2 Carbon black

Carbon black is one type of carbon allotropes. Overall image of its morphology is a group of thousands of spherical particles as called “agglomerate structure”. It is bound together with weak physical force or Van der Waals’ force between the smallest units of carbon black as called “aggregate structure or aciniform”. The aggregate structure is a micro-structure which consists of several individual spherical particles as called “primary particle”. It is fused together with strong chemical bond among the carbon elemen, Normally, the diameter of primary particles is in the range of 20–500 nm. Inside the primary particle is a mixing of amorphous carbon and micro-crystal of graphite-like structure. Especially, the micro-crystal structure on carbon black is a small imperfect graphite called “quasi-crystal”. Basically, these quasi-crystals of graphite-like structure have details about the length in a-axis (in plane) and c-axis (inter layer/crystallite height) which relate to their electrical properties, as shown in Fig. 2.3. In the molecular level of carbon black, hybridization of carbon atom is sp^2 on graphite-like structure and sp^3 on amorphous structure, thus the crystal structure is highly discontinuous or imperfect.

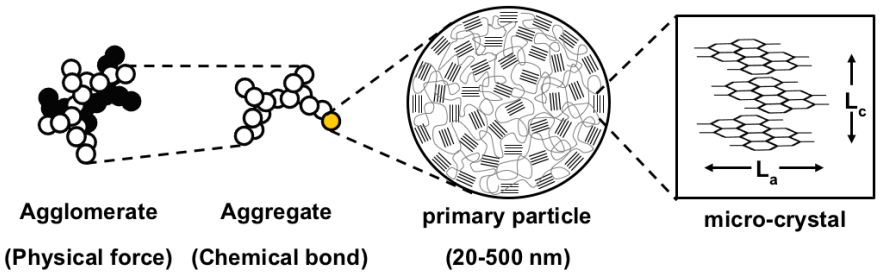

Fig. 2.3 The main structure of carbon black and soot.

In addition, Jean- Baptiste Donnet's review [10] showed the proposed resembling models of crystal arrangements inside the primary particle which were further improved using high resolution electron microscopy since 1956 to 1968, as below:

Sweitzcrct Heller 1956 | Donnet et Bouland 1963 | Donnet et Shultz 1965 | Heckman et Hardling 1966 | Hess. Ban et Heidenreich 1968

Fig. 2.4 Internal organization model of micro-crystals inside the primary particle of carbon black [10]. Copyright 1994 Elsevier Science Ltd.

As mentioned about the characteristics of carbon black, these structures cause interesting properties such as stability, high surface area, high electrical conductivity, *etc.* However, structure of carbon black is totally same as the morphology of soot, which is an undesired by- product from the combustion of fossil and biomass products. Soot is just a high environmental air pollutant which is released from various organic combustion engines converting 20% of the fuel to soot. Consequently, there are studies in difference between soot and carbon black in morphological and chemical structures and the difference is only the elemental compositions [11, 12], as shown on Table 2.1.

Table 2.1 Elemental composition of soot and carbon black [11].

Sample		Elemental composition, % wt									
		C	H	O	N	S	Ca	Zn	P	Fe	Other
Engine Soot		85.7	3		0.4		0.6	0.2	0.1		
		80.8		15.5	2.1	1.5					
		80.3	2.6		0.6						Na 0.3
		91.4	2		0.5						Na 0.3
		91.4	2.9	4.1	0.4	0.7	0.5	0.1	0.1		
		94.1	1.7	3.4	0.3	0.6					
		92.6	2.6	3.3	0.4	0.6	0.2	0.2	0.1		
		95	11.7	2.8	0.3	0.5					
Exhaust Soot		43.4	0.7		0.3	5.1	1.9	0.8	1	5.2	Mg 0.3
		51.4	0.7		0.3	5	2	0.9	1.2	7.8	Mg 0.3
Carbon black	Vulcan XC 72R	96.5	0.5		<0.1						
	Cabot fluffy	98.4		1		0.6					
	Regal 600	95.5	0.6	2.2	0.3	2.1					
	Flamruss 101	97.7	0.7		0.3						

While carbon black is nearly pure elemental carbon (>95 %wt), soot is high organic extract and heterogeneous substances depending on its source (carbon precursor, generating condition, lubricant composite, and oxidizing level of each system). Therefore, carbon black and soot have significantly different properties in usability and hazardous potential.

However, numerous models of this carbon particles formation have been studying in the incomplete combustion due to high awareness of environmental effect from soot. To understand the details of complex chemical reaction pathways for soot or carbon black formation, the experiments from carbon particle formation have been piled up.

In an incomplete combustion process, fuels or hydrocarbon materials are decomposed into radicals during heating and transformed to small molecules (especially, acetylenic species and aromatics) which create polycyclic aromatic hydrocarbon (PAH) species rising by the time. Until reaching supersaturated condition, the generated PAHs at low pressure condition initially condense and create the liquid nuclei which are more thermodynamically stable than free organic specie residues. Therefore, the nuclei are maintained and grown with the isolated species. At the same time, there are rapid polymerization with hydrocarbon radicals and formation of the building brick in the nucleus [13]. More graphitic structures are formed by changing aliphatic compounds to condensed aromatic ring, PAHs, or more graphitic structure due to high stability of graphitic form. There are two different types of carbon precursor as aromatic and aliphatic hydrocarbons. The aromatic precursors such as benzene, acetylene, naphthalene, and other molecules tend to form the active ring than aliphatic precursors and to make an excess of particle precursor circumstance leading tendency of soot generation. Some generated PAHs are desorbed to gas phase or laid on the particle surface, as shown in Fig. 2.5.

Several particles are rapidly coagulated and small radicals are taken up for surface growth with carbon-carbon bond at the same time [14,15]. It occurs in both individual particle and aggregate form for growing the individual particles and for stabilizing interval between two adjacent particles of aggregate structure, as shown in Fig. 2.6 [16].

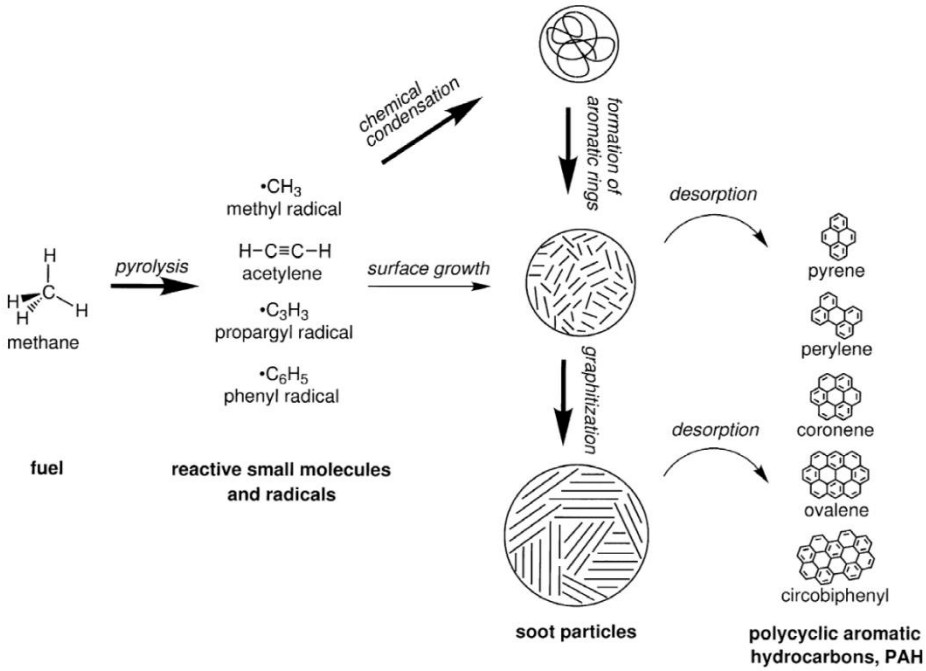

Fig. 2.5 Model of soot formation in an atmospheric pressure methane diffusion flame [14]. Copyright 2002 Elsevier Science B.V.

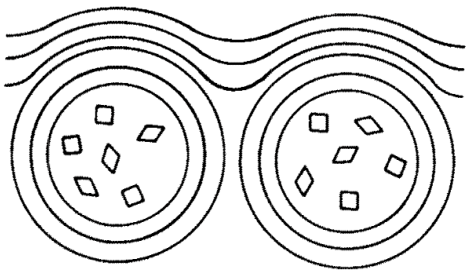

Fig. 2.6 Schematic of carbon layer from surface growth on individual and aggregate particles [16]. Copyright 1994 Elsevier Ltd.

Incomplete combustion and thermal decomposition are the main reaction of carbon black synthesis which are just different in oxygen existence. The oxidizing agents rise the oxidation level of carbon black which increases more acidity in their structures due to generation of oxygen functional groups [1]. Moreover, a rising of the oxygen functional groups decreases their electrical conductivity because they generate defects and vacancies inside the

layer of graphite and expands the intercalation of crystals of graphite-like structure [17, 18]. In the other hand, oxidizing system promotes the oxygen pitting on the particle structures which results to increase a specific surface area and porosity [1, 19, 20]. Carbon black produced by incomplete combustion is still essential to use as a printing ink, carbon electrode, and additive in elastomers owing to the properties of their functional group and others.

2.3 Synthesizing process of carbon black

Carbon black synthesis have 5 major methods of manufacturing which generate different characteristics (*e.g.*, primary particle size, specific surface area, adsorption capacity, and others using in), as shown in Table 2.2 for different applications. The process descriptions of all types are given below [1, 20].

Table 2.2 The chemical and physical characteristics of different manufacturing process [21]

Characteristic	Lampblack	Gas black	Furnace black	Acetylene black	Thermal black
Average particle size (nm)	110–120	10–30	10–80	32–42	120–500
Surface area (m^2/g)	16–24	90–500	15–450	65	6–15
DBP absorption (mL/100 g)	100–120	n.a.	40–200	150–200	37–43
Oil absorption (g/100 g)	250–400	220–1100	200–500	400–500	65–90
Color strength	25–35	90–130	60–130	n.a.	20
Volatile content	1–2.5	4–24	0.5–6	0.5–2	0.5–1
pH value	6–9	4–6	6–10	6–10	7–9

2.3.1 Lampblack process

Lampblack process is an first protocol to synthesize the carbon black as systematically. It has operated from a small scale to an industrial scale following the requirement at that time. In process, resin of plant or various organic materials are burned on large and shallow pan with incomplete combustion reaction inside the brick-wall of chimney to limit the oxidized agents or air. Synthesizing particles are generated, slowly floated and deposited on cold metal surfaces to break off the reaction. The synthesis parameters such as amount of air drawn by the suction at the end of reactor, heat energy by size of pan, and type of feedstock in the process were controlled. General properties of carbon black produced by this process are large size of primary particle, high structure, low surface area, very broad size distribution, unique color tone (blue), and ease of disperse. This black is used as a pigment and additive in rubber for mechanical applications. Even it is the oldest process, it is still carried out in Europe at present due to their unique properties.

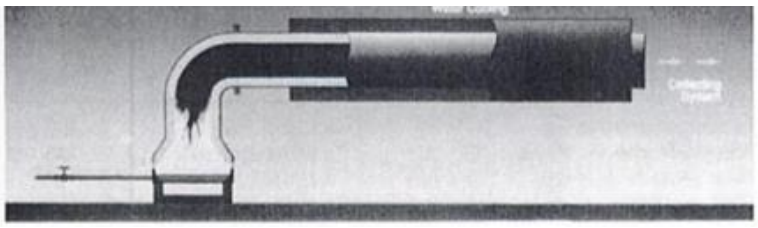

Fig. 2.7 Lampblack production plant.
Copyright 1993 MARCEL DEKKER, INC.

2.3.2 Gas and channel black process

Both gas black and channel black are generated through an incomplete combustion reaction using flames from organic materials in an open system (excess oxidizing agent). Carbon particles are formed and deposited on the surface of water-cooled iron channels (impingement) whereas a lot of free remaining particles are collected by filters. Gas black process is favored in Europe by using vaporized oil as raw materials while channel black process is favored in USA by using natural gas as raw materials. Gas black and channel black characters are low structure, high oxidizing degree, and small particle size which are suitable to be a reinforcing composite in rubber. In addition, gas black process which generally uses volatile oil for carbon black synthesis is convenient to adjust their carrier gas for manipulating the characteristic of synthesized carbon black. Therefore, the achieved particle sizes can be decreased to 10–30 nm. All general properties of this type together with smaller particle suit for a printing application.

(A) 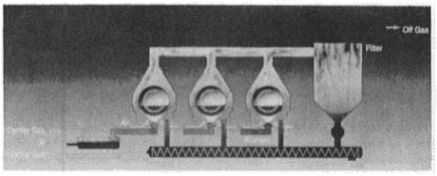 **(B)** 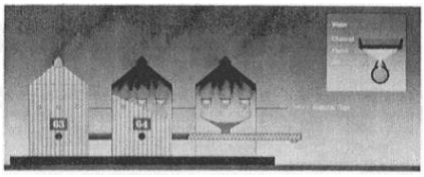

Fig. 2.8 Gas black (A) and channel black (B) production plant.
Copyright 1993 MARCEL DEKKER, INC.

2.3.3 Thermal black process

Thermal black process is operated using two refractory furnaces. The first is a heat generator which is processed *via* complete combustion of fuel using air and hydrogen gas. It is an energy source for next furnace. The second is carbon black generator where feedstock of precursor is converted to carbon black and hydrogen *via* thermal decomposition in the absence of air in every 5–8 min/cycle. Raw materials of thermal black synthesis are natural gas or liquid hydrocarbons. The off gas from the synthesis reactor carries out the carbon product to quenching system for decreasing temperature before filtered in separation part. 90% of hydrogen from waste gas is continuously used in heat cycle in the reactor. Owing to

synthesizing process, basic properties of thermal black are low oxygen content, the lowest surface area, the lowest structure, and the largest particle size about 500 nm, which produce high degree filler for polymer applications. However, thermal black is more expensive because of its unique physical properties (mechanical goods) for using in additive application of specific polymer such as O-rings and seals, hose, tyre inner liners, V-belts, and others.

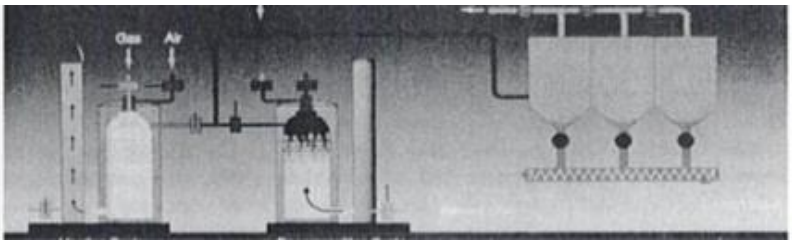

Fig. 2.9 Thermal black production plant.
Copyright 1993 MARCEL DEKKER, INC.

2.3.4 Furnace black process

Furnace black process is the most favor and modern process for carbon black synthesis due to a wide variety of uniform quality depending on the desire of product performance. This process uses both incomplete combustion and thermal decomposition reaction of organic hydrocarbon in closed reactors with continuous line production. There are 3 processing steps: the first is burning fuel to form combustion gas steam, the second is spraying feedstock through the combusted gas to do the reaction, and the last is quenching the carbon black process by water to terminate the reaction and collecting product by bag filter. Gas and oil hydrocarbon is used as raw materials forming different characters on the degree of structural complexity and impurity. Besides raw material types, this process is more flexible with the alternative controlling parameters such as temperature profile, pressure control, feed character, collecting technique, and reactor design. Moreover, this process is easy to modify and expand while their yield is high about 40–60 *%*.

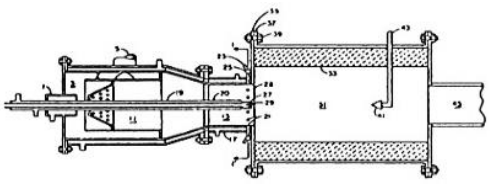

Fig. 2.10 Furnace black production plant.
Copyright 1993 MARCEL DEKKER, INC.

2.3.5 Acetylene black process

Acetylene black is a type of carbon black which is synthesized *via* thermal decomposition reaction of homogeneous feedstock as acetylene or acetylene precursor in

closed reactor with insufficient or absent amount of oxidizing condition (Eq. 1) at atmospheric pressure. In process, acetylene gas is continuously fed into the ordinary furnace or electrical furnace (closed reactor) by inert gas (mobile phase) and converted to carbon particles. Acetylene gas is easily activated and rapidly converted into carbon and hydrogen owing to their instability of triple bond in the chemical structure and their high positive free energy of formation. Finally, output product is cooled down and separated from the hydrogen tail gas.

$$C_xH_y \rightarrow C_n + C_{x-n}H_b + (y/2 - b/2)H_2 \qquad \text{(Eq. 1)}$$

The unique characters of acetylene black are pure carbon content about 92%, small primary particles, and high graphitization degree because of the condition of thermal decomposition, reaction rate, and high exothermic reaction of acetylene which are different from other feedstocks. As a result, acetylene black has excellence inherent properties such as high specific surface area, inert, hydrophobic, and especially high electrical conductivity. It is widely used in electronic applications (antistatic, electrical conduction, and energy storage), catalysis, pigment, and electrochemical analysis [1, 22, 23] which are specialty and high value application.

2.4 Graphitic structure

Main structure of acetylene black which differs from other types of carbon black is the high graphitic structure of graphite-like crystal. Graphite is a carbon structure in form of sp^2 hybridization to be the network of hexagonal structure like a honeycomb or graphene, as shown in Fig. 2.11 (A) and (C) stacked into the three-dimensional structure, as shown in Fig. 2.12. The remaining electrons in p orbitals or π bond are delocalized along bonds and atoms over the graphitic structure (Fig. 2.13) which provides the electrical conductivity on the graphitic structure [24]. In the case of defect crystals, as shown in Fig. 2.11 (B) and (D), the electron delocalization paths are discontinued. The electrical conductivity of this structure is dropped.

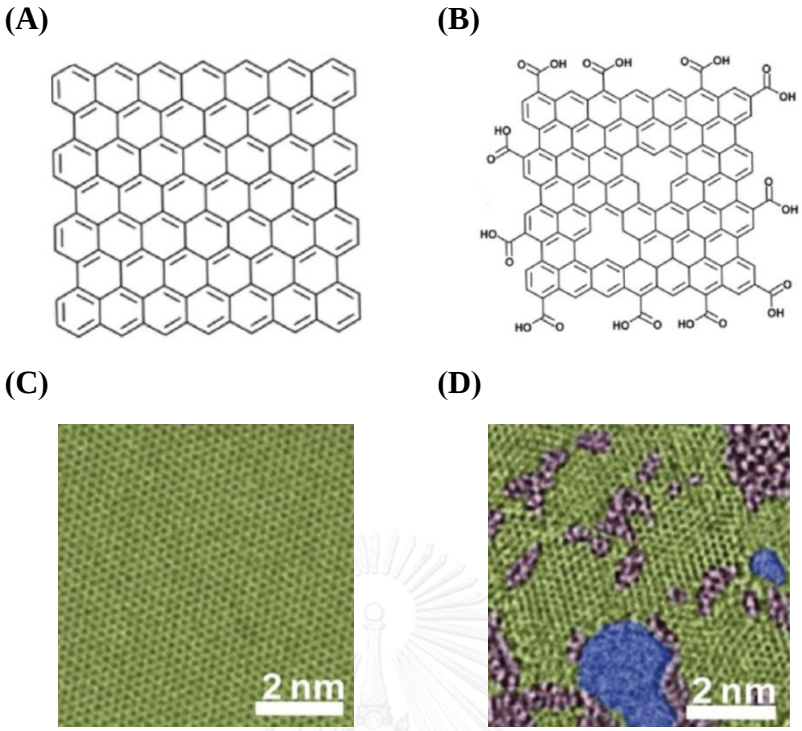

Fig. 2.11 Chemical structures of perfect graphene structure (A) and defected graphene with hole and functional groups (B) Color coded HRTEM images of perfect graphene structure (C) and defected graphene (D) [25]. Copyright 2012 Elsevier Ltd.

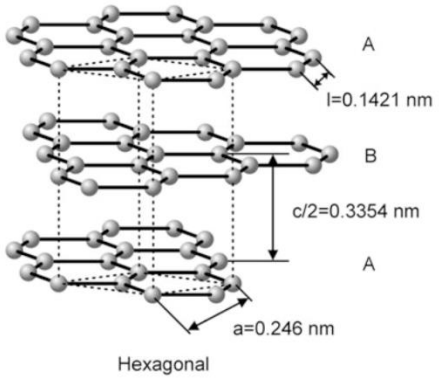

Fig. 2.12 The crystal structure of graphite [26].
Copyright 2016 Springer-Verlag Berlin Heidelberg.

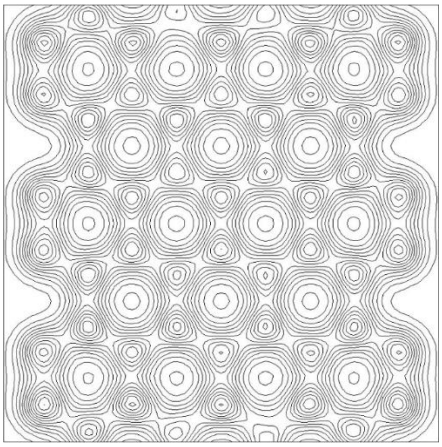

Fig. 2.13 Total electron density maps for graphite structure [27].

However, in the aspect of carbon black application, carbon black particles which compose of quasicrystal of graphite (imperfect crystal) have a suitable electrical property. The electrical mobilization inside individual particle and aggregate particle is still fine from the results of overlapping graphene layer [16], although it is not good as graphite structure.

2.5 Effect of acetylene black characters on their properties

Even though acetylene black is a carbon black grade which its field is specified on electronic application, using of it is variety in that field. Besides electricity, in use other properties, such as dispersibitlity, viscosity, reactivity, and others, also important as their electricity having suitable properties which totally cover is necessary.

2.5.1 Electrical conductivity

By following the predominantly electrical conductivity of acetylene black which depends on its chemical and morphological structures, numerous works studied the effect of its characters on electrical properties for conserving and developing electrical capability in individual or dispersing system. Firstly, polyaromatic characters inside carbon black particles are necessary for electrical conductivity which is proportional to the size of polyaromatic system [28]. Moreover, on the plane of graphite-like structure or polyaromatic system, the significant factor of electron transporting is the chemical functional group, hole, or non-carbon elements–the impurities on the graphitic plane–which constrain electron mobility or reduce the electron transport routes [29].

As mentioned about the electron mobilization on the aggregate structure (2.4), the problem of electrical conductivity in carbon black always results from the distance between adjacent of particles which are increased when carbon black is dispersed for any application

[16]. For functional groups on particle surface, besides including of oxygen and hydrogen atoms localize the electron mobility, C–C bond in carbon black may be broken to promote the reaction and form bond with the dispersing metric (polymer) during the process with the presence of impurity [29].

Thirdly, the study about effect of aggregate structure in polymer environment (polymer composite) on polymer properties showed that when structures are high degree of aggregation, the electron mobility between aggregate particles and the universal percolation-network geometry (homogeneous properties) are increased. Due to the distance between adjacent aggregate particles and the distribution are decreased, as shown in Fig. 2.14 [30].

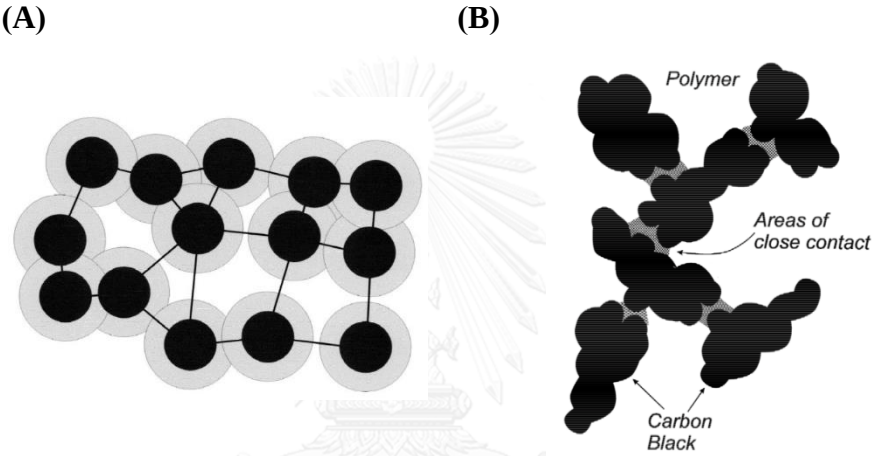

Fig. 2.14 An illustration of almost close-packed network of low structure (A) and high structure of aggregate particles (B) [30]. Copyright 2002 Elsevier Science B.V.

On the contrary, some works studied on carbon black by measuring the electrical resistance when the pressure was raised. The high structure carbon black which has low density has lower electrical conductivity due to high non-contact between particles and low orderliness of the packing than low structure carbon black which is in the closed packing form [31].

In primary particle aspect, the smaller particles which trend toward smaller size of aggregate lead to smaller gap and more conducting routes as previously mentioned [29].

2.5.2 Vulcanization and reinforcement properties

Because of suitable properties of carbon black (*e.g.* low density, hydrophobicity, dispersibility, and others), it is usually applied in polymer and rubber industry which mainly use non-polar materials. Carbon black always has a physical crosslink with uncured polymer before vulcanization and has a chemical bonding after vulcanization. In addition, the sulfur residues on carbon black surface consider as the active group during vulcanization. Therefore, carbon black which has high specific surface area is inevitably increased polymer mechanical

properties before and after vulcanization. However, it decreases the elongation at break (flexibility) [32] .

2.5.3 Dispersion

To use carbon black in any application, good dispersion and homogeneous mixture are always needed for generating full and consistent efficiency with low mechanical force. Dispersibility of carbon particle depend on the structural degree. The high structures of aggregates also have a high degree of attractive force which is hard to separate because of more interactions with neighbors. Accordingly, the low structures of carbon black are more easily dispersed [33] . Besides the morphology aspect, the chemical property which is the main character of surface energy is essential for the adhesion force between solute (filler) and solvent (polymer or other metrics). If both surface energies become closer, dispersion of carbon black is promoted [34] .

2.5.4 Viscosity

The relation of filler and surrounding media is the key of rheology or viscosity property. The media which tightly adsorbs on filler surface with high area of interaction generally encourages the viscosity value. Therefore, viscosity is proportional to the specific surface area of carbon black [34].

2.6 Characterization techniques

2.6.1 Raman and IR spectroscopy

Theory of both Raman and IR spectroscopy involve about interaction of radiation on molecular vibration which is used to be analytical technique for elucidating the molecular structure by characteristics of fundamental vibration of each molecule. Each vibrational character has differently active and inactive in Raman or IR mode, due to differential process and selection rules. Raman and IR spectra characters indicate energy, polarizability/dipole moment, and bond environment by wavenumber, intensity, and band distribution, respectively, so they usually used to identify the molecular structures and functional groups.

IR spectra are originated by changing of dipole moment of activate molecules, but Raman spectra are originated by changing of polarizability. Therefore, IR spectroscopy is favored in asymmetric vibrations of polar groups whereas Raman spectroscopy is favored in symmetric vibration of non-polar groups [35].

In contrast, the results of IR and Raman spectra on the lattice vibration are illustrated by the selection rules. For carbon materials analysis, irreducible representation of graphite structure (point group*:* D_{6h}) is presented as follows [36]:

$$\Gamma_{opt} = 2E_{2g} + E_{1u} + 2B_{2g} + A_{2u} \qquad \text{(Eq. 2)}$$

The different structures as single layer (2D structure) and multilayer (3D structure) relate to intermolecular interaction existence which induces the Davydov splitting on their modes of graphite structure to differ from graphene layer, as shown in Fig. 2.15.

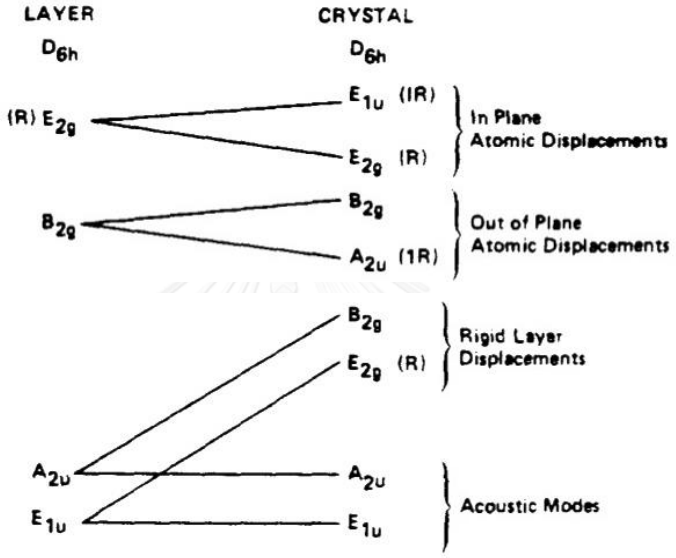

Fig. 2.15 The illustration of vibration mode of single and multilayer graphite [36].
Copyright 1977 Elsevier Ltd.

By changing to 3D structure, E_{2g} and E_{1u} phonon of 2D structure are divided into E_{2g} (Raman-active) and E_{1u} (IR-active) while B_{2g} phonon and A_{2u} phonon of 2D structure are divided into B_{2g} and A_{2u} (IR-active). From the irreducible representation, the different optical modes of atomic displacement of graphite structure, as shown in Fig. 2.16, are different patterns in atomic movement as in plane, out of plane, rigid layer and acoustic mode. The different chemical structures are characterized by cooperating with Raman and IR spectroscopy.

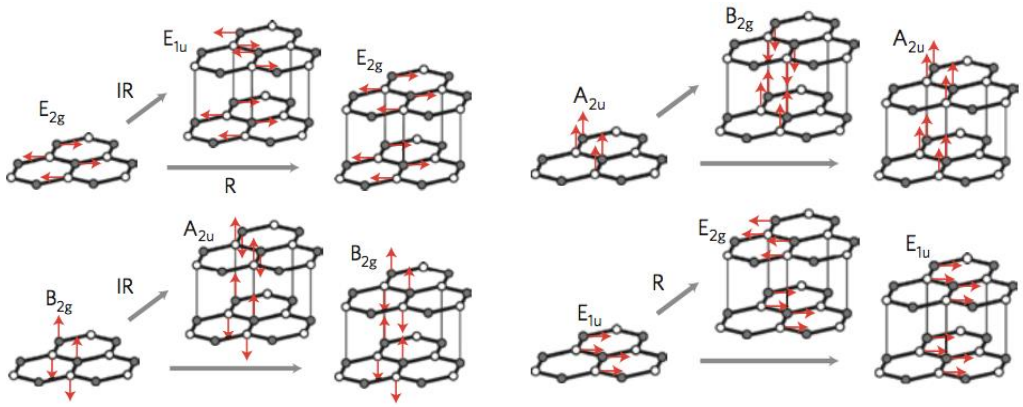

Fig. 2.16 The atomic displacements of atom in graphitic [37]. Copyright 2013 Rights Managed by Nature Publishing Group.

2.6.2 XRD (X-ray diffraction) and Raman spectroscopy for the crystal measurement

Basically, XRD technique is normally used to analyze the spatial arrangements of atoms between 10^{-10}–10^{-6} m in crystal structure from bridging of the unit cell. To investigate the crystal structure, geometrical relationship of wave interference is converted to the diffraction pattern of material. However, this technique is used to analyze the amorphous structure. In the case of defect or disorder materials, their diffraction patterns are relatively broad and weak.

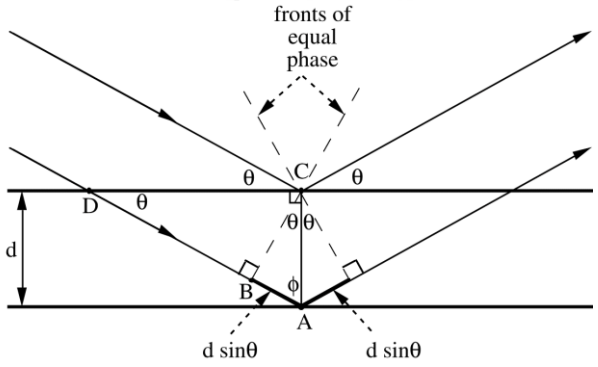

Fig. 2.17 Schematic of wave scattered interference of two parallel rays at planes of crystal structure [38]. Copyright 2013, Springer-Verlag Berlin Heidelberg.

To elucidate the diffraction pattern, wavelength of incident rays is compared to the spacing between atoms on such crystallographic plane. Fig. 2.17 shows that the different path length of the scattering ray at the top plane and the bottom plane equals to 2dsinθ. Each distinct peak in diffraction pattern exhibits a different interplanar spacing (d), and the diffraction

patterns also exhibit all spatial atomic arrangements of such material. The average spacing between atom is estimated by Bragg's equation [38].

$$2d\sin\theta = n\lambda \qquad \text{(Eq. 3)}$$

when d is the interplanar spacing, θ is the scattering angle, n is the reflection order (integer), and λ is the wavelength of incident wave.

In XRD measurement on graphitic structure (hexagonal structure), (10ℓ) and (002) crystal planes are used to represent graphitic plane in a- and c-axes, respectively. More information of crystal planes at (10ℓ) and (002) and graphitic structure are given in Fig. 2.18.

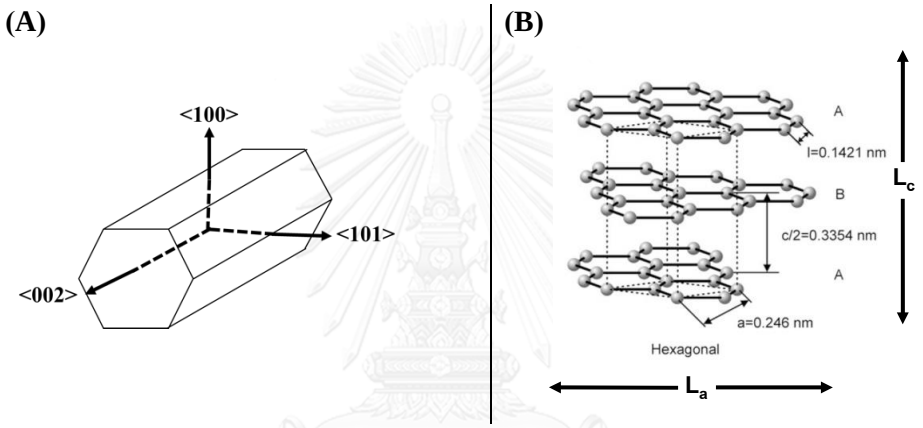

Fig. 2.18 Schematic of Crystal planes of hexagonal cell at (100), (101), and (002)(A) [39] and graphitic crystal (B)[26]. Copyright 2015 Springer-Verlag Berlin Heidelberg. Adapted with permission.

XRD technique is used to determine the plane size of crystals (a- and c-axes) *via* Scherrer's equation [40, 41].

$$L_i = \frac{K_i\lambda}{B_i\cos\theta_i} \qquad \text{(Eq. 4)}$$

when L is the calculated value of average size in any axis of crystals (nm), K is a constant which is 1.84 for peak of (10ℓ) plane (a-axis) and 0.89 for peak of (002) plane (c-axis), λ is the X-ray wavelength which is 0.154 nm for Cu-K_α radiation, B is the full width at half maximum (FWHM) of a relevant peak, and θ is the scattering angle.

In addition to XRD technique, many works tried to develop capability of Raman spectroscopy to indicate the crystal size of graphite-like structure (especially carbon black samples).

In Raman spectral analysis of carbon materials, there are 4 peaks position at 1165, 1310, 1485, and 1590 cm^{-1}. Two peaks at 1165 and 1485 cm^{-1} are peak characters of amorphous

carbon [42] and amorphous carbon at interstitial place [43], respectively, whereas other two peaks at 1310 and 1590 cm^{-1} are peak characters of edge of graphite crystal (D; disorder) and graphitic structure (G; graphitic), respectively [44]. Therefore, the peaks at 1310 cm^{-1} (D) and 1590 cm^{-1} (G) are considered for crystal size calculation in a-axis (in plane of graphitic structure).

Initially, Tuinstra and Koenig [45, 46] studied the relation of intensity ratio of Raman spectra and L_a values, which are measured from XRD. The L_a value depends inversely on the ratio of I_D/I_G and empirical formula is given by

$$L_a = 4.35\left(I_D / I_G\right)^{-1}(nm) \quad \text{(Eq. 5)}$$

when L_a is the calculated crystal size of a-axis (nm), I_G is the intensity of G band (at 1600 cm^{-1}), and I_D is the intensity of D band (at 1350 cm^{-1}) by using an excitation laser of wavelength at 488 nm.

Previously, several works of carbon black used Tuinstra's equation for calculating the mean of crystal sizes in a-axis length being higher than 4 nm. However, few current studies showed a contrary relation with previous works. When the samples are higher amorphous (sp^3), the ratio between I_D/I_G are varied with the crystallite sizes of samples, as shown in Fig. 2.19.

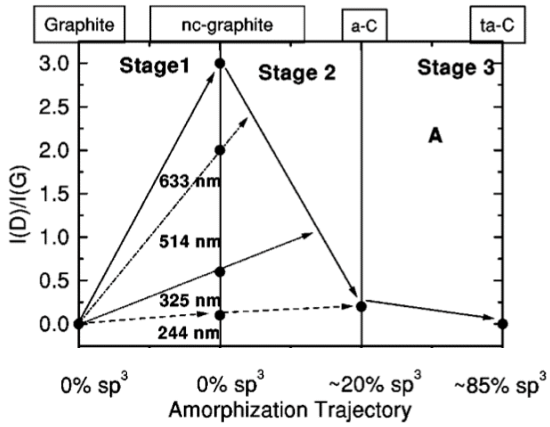

Fig. 2.19 The relation between ratio of I_D/I_G and amorphization trajectory at different excitation wavelength [47]. Copyright 2001 American Physical Society.

Ferrari and co-workers studied in depth of the relation of I_D/I_G intensity ratio and the distance between defects (L_D) in plane (a-axis) preparing by ion bombardment on graphene, which is the most favored material in research topics at the moment, over the range of plane sizes (0–30 nm), as shown in Fig. 2.20.

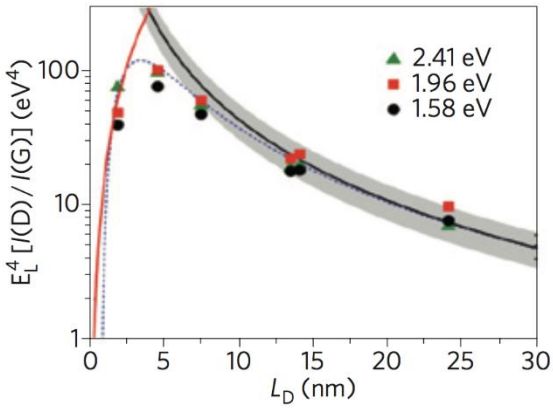

Fig. 2.20 The plot between $E^4_L[I_D/I_G]$ and L_D at different excitation energies, E_L [37]. Copyright 2013 Nature Publishing Group.

The mean sizes of L_D which are smaller than 3 nm are calculated by Eq. 6 from the fitting in red line of this experiment data [37].

$$L_D^2(nm^2) = 5.4\times10^{-2} E_L^4(eV^4)\frac{I_D}{I_G} \qquad \text{(Eq. 6)}$$

when L_D is the calculated distance between defect in a-axis (nm), E_L is the laser energy (eV) which is 2.3308 eV (780 nm wevelength), I_G is the intensity of G band (at 1600 cm^{-1}), and I_D is the intensity of D band (at 1350 cm^{-1})

In carbon black studies, the calculated crystal sizes are focused on the range of size which is lower than 3 nm because the range between 1–3 nm is normal size for the synthesized carbon black without pre- or post-treatment [43, 48, 49].

2.6.3 Nitrogen adsorption-desorption (adsorption isotherm)

Nitrogen adsorption-desorption is an analytical technique using the physisorption process of molecules of nitrogen gas on solid surface. Molecules of gas are filled to adsorb on the surface of sorbent materials and returned to desorb from that surface again for observing the dynamic or adsorption equilibrium by measuring the change of nitrogen gas pressure at 77 K. Surface characters such as pore size, surface area, adsorption behavior, *etc.* are analyzed with calculation methods, for instance, Brunauer–Emmett–Teller method (BET), Langmuir, and others which depend on their adsorption-desorption phenomena observing by the adsorption-desorption isotherm. Adsorption-desorption isotherm is a relation between relative pressure and volume of adsorbate. Fig. 2.21 shows 6 different types of adsorption-desorption isotherm classified by IUPAC recommendation.

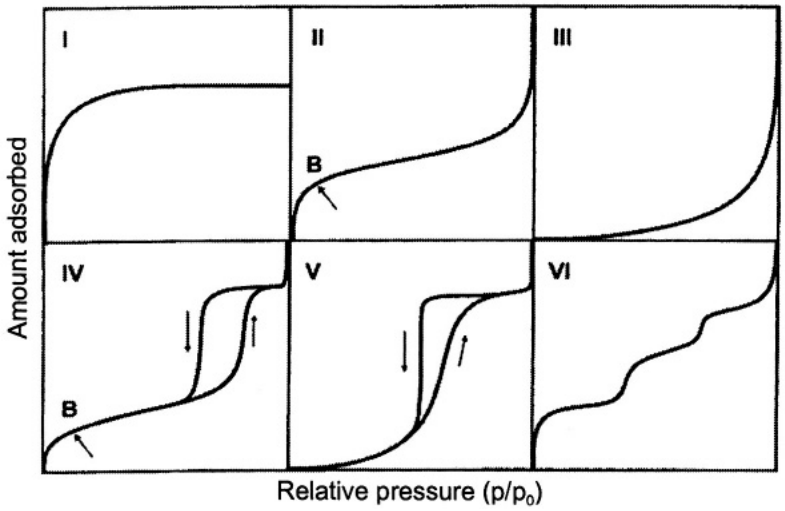

Fig. 2.21 General types of adsorption isotherm [50].
Copyright 2005 Springer Science and Business Media.

Type I isotherms are characteristic of monolayer adsorption and microporous materials. The adsorption maybe chemisorption system from monolayer adsorption which can be described by the Langmuir equation [50].

Type II isotherms are characteristic of mesoporous, nonporous, or only macroporous solids. (pore diameter > 50 nm). Their adsorption is monolayer at low pressure and multilayer at high pressure. The adsorption can be described by the BET equation for multilayer character [50].

Type III isotherms describe an adsorption character which the interaction between adsorbate and adsorbent is weak [50].

Type IV isotherms are adsorption behavior of microporous in mesoporous. The hysteresis loop refers to the capillary or bottle neck which desorption behavior is not same as adsorption [51].

Type V isotherms describes of small interaction between adsorbate and adsorbent, but their character presence of mesoporous structure with the capillary crack which induces hysteresis loop phenomena [51].

Type VI isotherms are adsorbed with stepwise multilayer of nonporous substrat [51].

CHAPTER III

EXPERIMENTAL

3.1 Materials

Acetylene gas (99.6%), nitrogen gas (99.999%), and liquid nitrogen (99.998%) were purchased from Praxair (Thailand) Co., Ltd. Ethanol (A.R. Grade) was purchased from Merck Ltd., Thailand. Polyvinylpyrrolidone (PVP) K90 was purchased from a commercial source. All chemicals were used as received without further purification. Filter (No.1, ID 125 mm, and particle retention ≥11 μm) was produced by Whatman®.

3.2 The synthesis of acetylene black

Acetylene black was synthesized *via* pyrolysis reaction of acetylene under nitrogen atmosphere using a homemade electrical furnace reactor at atmospheric pressure. The schematic drawing of this reactor is shown in Fig. 3.1. There are three main parts of reactor consisting of a feedstock control, an electrical furnace, and a collecting system. Electrical furnace consists of three longitudinal heating parts and three longitudinal points of temperature measurement involving R-type (-50–1480 °C), B-type (0–1700 °C) and R-type thermocouple, respectively, to obtain equally axial temperature distribution. The synthesis parameters of temperature (950–1300 °C), acetylene concentration (10–70 %v/v), and residence time (3.5–22.2 s) by adjusting flow rate (0.6–3.8 L/min) were varied to study their effects on synthesized acetylene black.

Firstly, nitrogen gas (0.7 L/min) was continuously fed from a feedstock control into an alumina tube (1.68 cm ID and 100 cm longitudinal length), which was placed inside the furnace, to gently heat up the reactor and remove other existing gases (oxidizing agents or other impurities). The furnace was heated with 15 °C/min with flow of nitrogen for 1.5 h to get the desired temperature. For preparing the concentration and flow rate of acetylene, acetylene gas was mixed with nitrogen gas (as a mobile phase and a diluent) in desired volume homogeneously. After that, the gas mixture was fed into the reactor continuously. Acetylene black was initially produced inside the heated alumina tube, and then flowed out from the reactor tube. Flowing gas was bubbled into the 500 mL DI water (7 cm height) for 2 cycles in a closed bottle to collect carbon particles. Acetylene black in water was filtrated using filter paper and dried at 70 °C in an oven for 3 h. An acetylene feedstock was fed for 2–12 min

depending on each condition to theoretically achieve a carbon product of 1.2 g from calculation in all experiments.

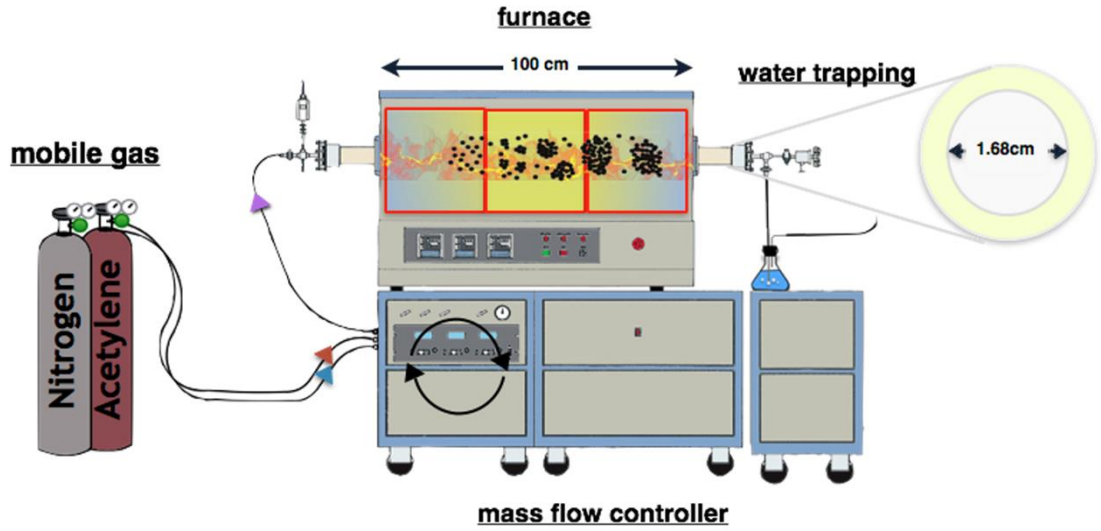

Fig. 3.1 Schematic drawing of the electric furnace reactor.

3.3 Characterizations

3.3.1 Morphological characterizations

3.3.1.1 Scanning electron microscope (SEM)

External morphology and particle sizes of acetylene black were observed by SEM (JEOL JSM-6510A) with an accelerating voltage of 10 kV using secondary electron imaging (SEI) mode. For a sample preparation, a few milligrams of synthesized acetylene black were totally dispersed in ethanol using ultrasonic processors (Sonics VCX-750 Vibra Cell) with power 225 watts and 1 s pulse on and 2 s pulse off for 1 min of working time), and then the acetylene black suspension was dropped on a silicon wafer stuck on an aluminum stub with carbon tape and spin-coated to spread aggregate particles of acetylene black. To eliminate the remaining ethanol, the sample on the stub was evacuated for 15 min. The diameter of the primary particles was determined using ImageJ software. In each condition, 300 individual particles were measured from different SEM images.

3.3.1.2 Dynamic light scattering (DLS)

Aggregate size of acetylene black was determined by DLS (Mastersizer-3000) and calculated by Mie scattering theory. Each sample was suspended in 10 mL ethanol and sonicated using ultrasonic processors (300 watts and 1 s pulse on and 2 s pulse off for 1 min of working time) in order to break their agglomerate structures and get the suspension of

individual aggregate particles. For decreasing flocculation problem of aggregate particles during the whole time of measurement, this suspension was stabilized with 10 mL of 10 %w/v PVP (K-90) in ethanol and sonicated with the same setting frequency 40 s working time. The solution was diluted with 1 L of DI water and continuously sonicated with the same setting frequency for 15 s. Particle reflective index of samples was set at 2.420 and 1.840 (only the study of concentration parameter in a different time) for calculation.

3.3.1.3 Nitrogen adsorption-desorption analyzer

All samples (approximately 40 mg) were degassed at 300 °C for 3 h by Belprep-vac II (BEL Japan, Inc.). External surface area and porosity of acetylene black were measured by nitrogen adsorption-desorption analyzer (BEL Japan, Inc. Belsorp-mini II analyzer) at -195.8 °C with high purity nitrogen (99.998%) and calculated by the Brunauer-Emmett-Teller (BET) method.

3.3.2 Chemical and crystallinity characterizations

3.3.2.1 Fourier-transform infrared (FT-IR) spectrometer

Infrared spectra of acetylene black were collected by Nicolet 6700 FT-IR spectrometer coupled with Continuμm IR microscope and a home-made slide on dome-shaped germanium internal reflection element (Ge IRE) for attenuated total reflection (ATR) mode. IR source was the standard Globar TM infrared light source with 100 μm aperture. All samples were scanned with 4 s exposure time and 64 number of scans. The signal was detected by mercury-cadmium-tellurium (MCT) detector. All samples were prepared by squeezing sample powder on a foil-covered glass slide. IR spectra were received from 3 different positions of each sample with a resolution of 4 cm^{-1} in the spectral range of 4000–700 cm^{-1}.

3.3.2.2 DXR Raman microscope

Raman spectra of acetylene black were recorded using DXR Raman microscope (Thermo Scientific) with 780-nm excitation laser (0.7–1.2 mW laser power) using 4 s exposure time and 64 numbers of scan, 25-μm aperture slit, and 50x-objective were employed with a laser spot size of 1 μm and a spectral resolution of 4 cm^{-1}. Each sample was measured from 3 different positions. Sample preparation was the same as IR measurement.

Raman spectra were fitted by using OMNIC program to extract all component peaks. A baseline correction was performed in the range between 1900–800 cm^{-1}. Each spectrum was smoothed to decrease noise. Savitzky-Golay second derivative with 51 points and 3 polynomial order were used to find the accurate peak positions of overlapping peak components which

were averaged from 3 spectra in each sample. Raw pattern of XRD was performed with Voigt-type line-shape. In addition, for graphite-like structure measurement (crystal size in a-axis), intensity ratio from resolved peaks was measured and calculated using Ferrari's equation [37].

3.3.2.3 X-ray powder diffractometer (XRD)

The micro-crystal size of graphite-like structure in acetylene black was determined with X-ray diffractometer (Rigaku Model: D/MAX-2200 Ultima^{+} diffractometer). Cu-K_{α} radiation (λ = 0.154 nm) was used as an x-ray source which was operated at 40 kV and 30 mA with slit parameters of DivSilt = SctSlit = 0.5°, RecSlit = 0.3 nm, and DivH.L.Slit = 10 mm at room temperature. X-ray detector was the scintillation counter which was mounted on the goniometer and moved over the angular range 2θ of 10–60° with a scan rate of 2°/min and a sample width of 0.02°.

Mean crystal size was calculated from FWHM of each peak using Scherrer's equation [41]. Prior to measure the FWHM to calculate the L_a value, XRD patterns were smoothed using 200-point Savisky-Golay smooth and 2-polynomial order before.

CHAPTER IV

RESULTS AND DISCUSSION

In this chapter, the effects of synthesis parameters, *i. e.* , temperature, acetylene concentration, and residence time on the morphological and chemical structure of synthesized acetylene black were studied. Acetylene black characters were elucidated using analytical methods from specific instruments. Morphology of acetylene black was investigated by SEM, DLS, and nitrogen adsorption–desorption while chemical structure of acetylene black was investigated by IR spectroscopy, Raman spectroscopy, and XRD.

4.1 Effect of temperature on acetylene black synthesis

Acetylene black samples were prepared by varying furnace temperatures from 950 to 1300 °C. The acetylene concentration was 10 %v/v and the residence time of precursor in the reactor was 13.3 s.

4.1.1 Effect of synthesis temperature on morphology of acetylene black

By using the synthesis temperature of 950 °C, acetylene was initially changed to carbon materials, which were roughly observed from their external appearance by naked eye. The product was fine black powder while it produced yellow color stained on its plastic container. This yellow stain indicates the formation of tar and volatile organic compounds, which are unwanted by-products retained inside the carbon materials. This organic residues or high hydrogen composite residues reduce carbon black efficiency, *i.e.*, electrical property [29]. The synthesis was also performed at higher temperatures to study the effect of temperature on acetylene black synthesis, which the yellow stain was not further observed.

External morphology of acetylene black in micro-scale was revealed by SEM and the diameter of their primary particle was measured by ImageJ program. From SEM images (Fig. 4.1), the morphology of acetylene black is aggregate of several spherical particles which are the simple form of carbon black. Their diameters of primary particles seem to decrease with an increase in the synthesis temperature.

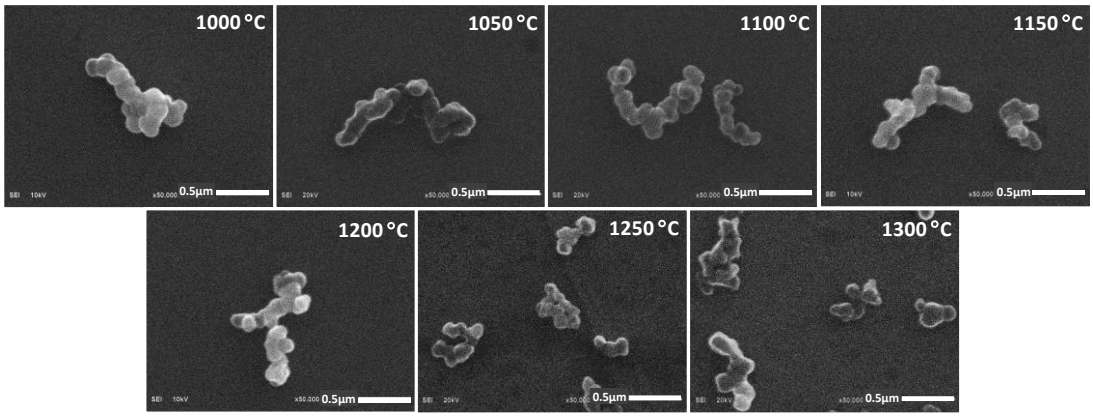

Fig. 4.1 SEM images of acetylene black synthesized at different temperatures (using an acetylene concentration of 10 %v/v and a residence time of 13.3 s).

By measuring the particle size from SEM images, particles size distributions of primary particles (Fig. 4.2) and plot of diameter of primary particles at different temperatures (Fig. 4.3) reveal that the primary particle diameter was considerably decreased from 174 ± 20 nm to 107 ± 18 nm with an increase in temperature from 1000 °C to 1150 °C. At higher temperatures (1150–1300 °C), the small increase in particle size between 107 ± 18 nm and 90 ± 21 nm is observed.

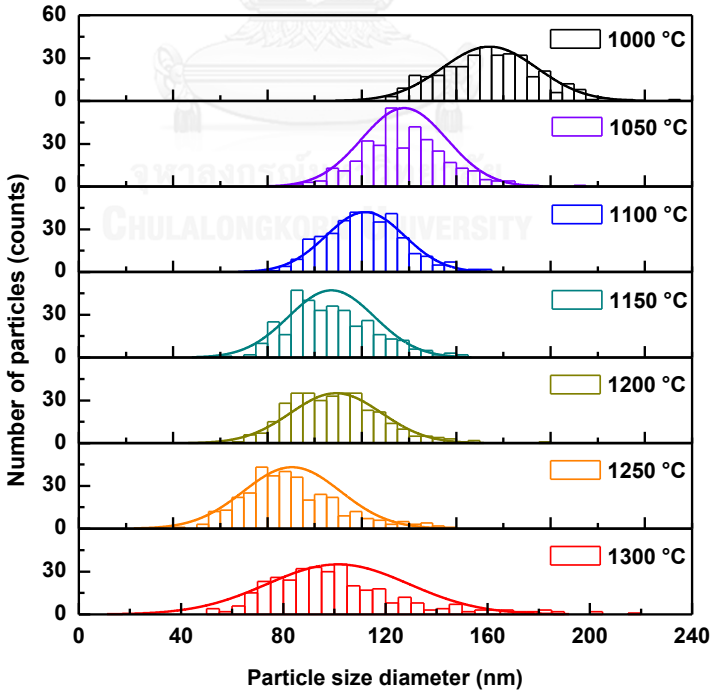

Fig. 4.2 Particles size distributions of primary particles of acetylene black synthesized at different temperatures (using an acetylene concentration of 10 %v/v and a residence time of 13.3 s).

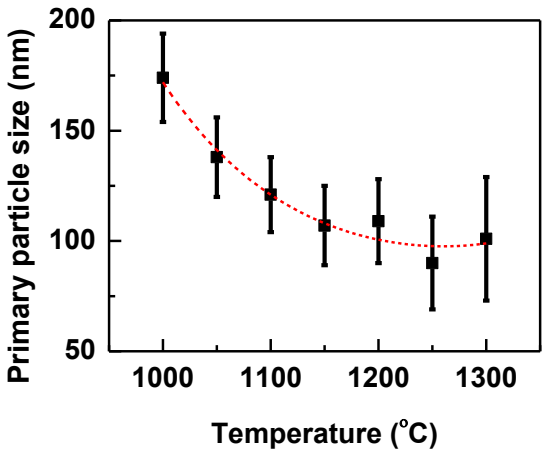

Fig. 4.3 Plot between primary particle size and synthesis temperature (using an acetylene concentration of 10 %v/v and a residence time of 13.3 s).

It seems that the rise of synthesis temperature significantly affects and decreases the primary particle sizes of acetylene black. Primary particle size gradually constants with small fluctuation when synthesis temperature is over 1150 °C. Carbon nucleation is used to describe these results. Initially, acetylene is immediately dehydrogenated and changed to polycyclic aromatic hydrocarbons (PAHs) which induce the seeding phenomenon until the system is totally saturated with the nuclei precursor. Then, the nuclei are suddenly generated [52]. An increase in temperature raises the number of active carbonaceous species as large polycyclic aromatic hydrocarbons (LPAHs) structures which are rapidly and highly converted to a great number of nuclei or seed at the initial state [49]. Next, a small amount of the precursor or hydrocarbon residues deposits on the nuclei surface and induces primary particles to form larger particles. On the other hand, the number of LPAHs is reduced when the reaction occurs at low temperatures, and then it is replaced by small polycyclic aromatic hydrocarbons (SPAHs) which pushe the surface growth of particle as followed in Fig. 4.4.

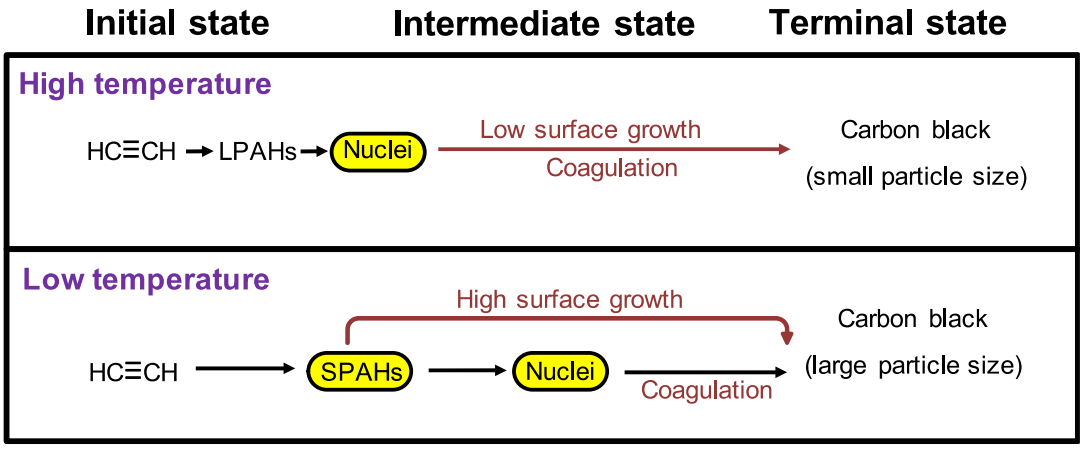

Fig. 4.4 Flow of life time for acetylene black intermediate at low and high synthesis temperatures [49].

From SEM data, the effect of rising synthesis temperature on particle sizes, which induces a decrease in particle size, could infer that the surface area of acetylene black will also increase. To ensure the temperature effect on their porosity and surface area, nitrogen adsorption–desorption was used to investigate the adsorption isotherm and specific surface area.

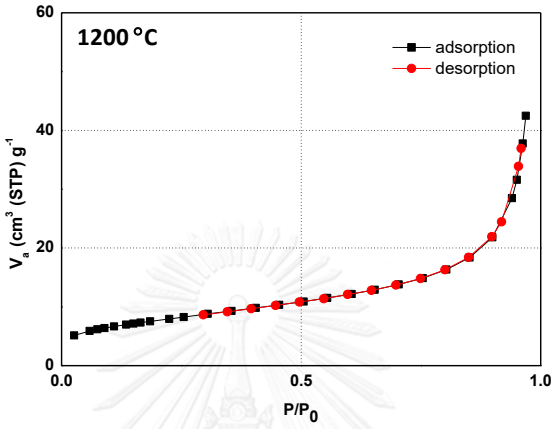

Fig. 4.5 Adsorption-desorption isotherm of acetylene black synthesized at 1200 °C (using an acetylene concentration of 10 %v/v and a residence time of 13.3 s).

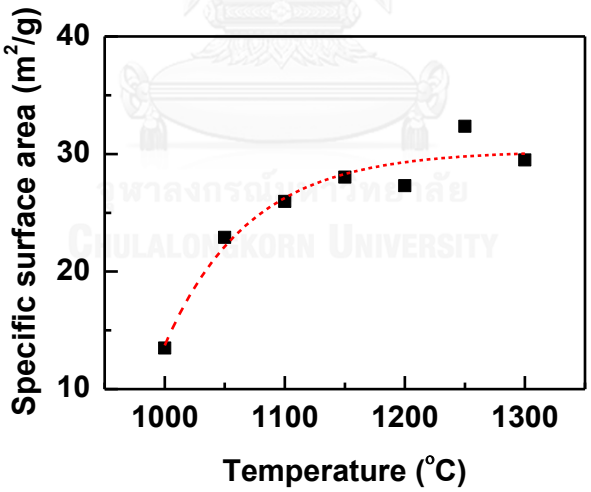

Fig. 4.6 Plot of specific surface area against synthesis temperature (using an acetylene concentration of 10 %v/v and a residence time of 13.3 s).

Fig. 4.5 shows the adsorption-desorption isotherms of acetylene black synthesized at 1200 °C as type II which reveals a nonporous structure. In addition, This isotherm represents for all samples in same character. Therefore, this synthesis system used thermal decomposition reaction which did not have oxidizing agent for carbon removal generating porosity [1, 19]. BET calculation was used to determine the specific surface area of carbon particles. From Fig. 4.6, the specific surface area is obviously increased from 13.49 to 28.03 m^2/g with an increase in temperature from 1000 to 1150 °C. However, at higher temperatures, the specific surface area is slightly fluctuated. It coheres to the SEM data which their particle size is proportional to their surface area.

SEM images (Fig. 4.1) show the individual unit of acetylene black or aggregate structure as various sizes and structures. At high synthesis temperatures, their aggregate sizes also seem to be small. However, measuring aggregate sizes using SEM images was inconvenient and may receive an inaccurate data from small population of SEM samples. Thus, dynamic light scattering technique (DLS) was used to investigate aggregate sizes with larger sample population.

Acetylene black was totally suspended in ethanol and examined by DLS technique for measuring an aggregate size. The size distributions of aggregate particles synthesized at different temperatures from DLS measurement are shown in Fig. 4.7.

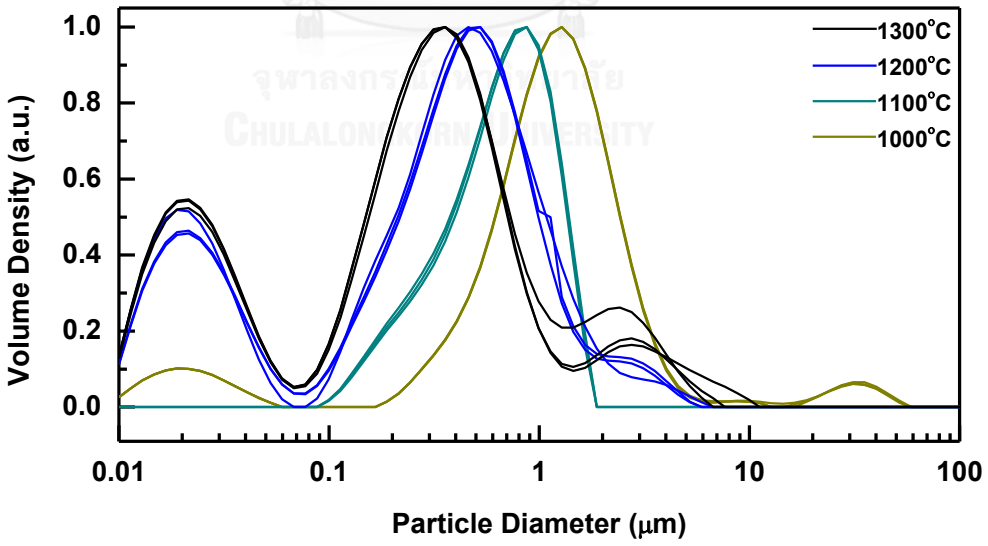

Fig. 4.7 Particles size distributions of acetylene black synthesized at different synthesis temperatures (using an acetylene concentration of 10 %v/v and a residence time of 13.3 s).

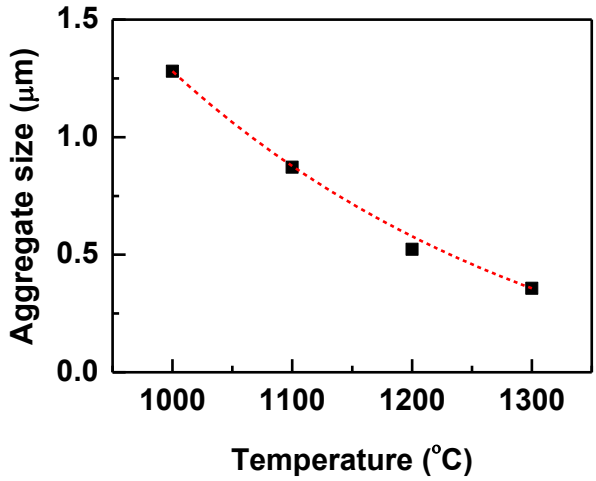

Fig. 4.8 Plot between aggregate size of acetylene black and synthesis temperature (using an acetylene concentration of 10 %v/v and a residence time of 13.3 s).

The plot between maximum population size of aggregates and synthesis temperature (Fig. 4.8) shows that aggregate size is also decreased from 1.280 to 0.357 μm by increasing temperature from 1000 to 1300 °C. This is similar to the result of temperature effect on their primary particle. The effect of temperature on aggregate sizes strongly depends on their primary particle size. Firstly, their smaller unit (as primary particle) is varied in line with the aggregate particles. Secondly, before aggregation, smaller primary particles, which have higher surface energy than larger primary particles [53], are induced to aggregate together to loss their active surface area directly relating to an excess surface energy [54]. Thus, the aggregate particles of small primary particles may be close packing (small aggregate particle diameter) to reduce their surface more than that of larger primary particles which tend to bind together in linear form (large aggregate particle diameter).

4.1.2 Effect of synthesis temperature on chemical structure of acetylene black

In acetylene black synthesis, thermal decomposition reaction consumes heat energy to drive the formation of carbon structure. Generally, this formation prefers to be a graphite structure due to a thermodynamically stable carbon form [7]. However, the molecular structure of acetylene black is a mixture of sp, sp^2 and sp^3-hybrid carbons (a main composition) with a small part of hydrogen element. It leads to a formation of crystalline and amorphous phases in carbon particles. In this part, we studied on the chemical structure of acetylene black including the whole information of molecular structures, crystallinity, and functional groups of acetylene black by using techniques of Raman spectroscopy, XRD, and FT-IR spectroscopy.

Firstly, the effect of temperature on crystal structures was studied using XRD technique. Fig. 4.9 (A) shows an XRD pattern of acetylene black synthesized at different temperatures. Two band at 23.0° and 43.5° correspond to (002) and (10ℓ) plane in crystal lattice of carbon element, respectively [41]. The crystals size on a-axis dimension of graphite like structure (L_a) was analyzed from peak position and full width at half maximum (FWHM) of the band at 43° (10ℓ plane) by using Scherrer's equation.

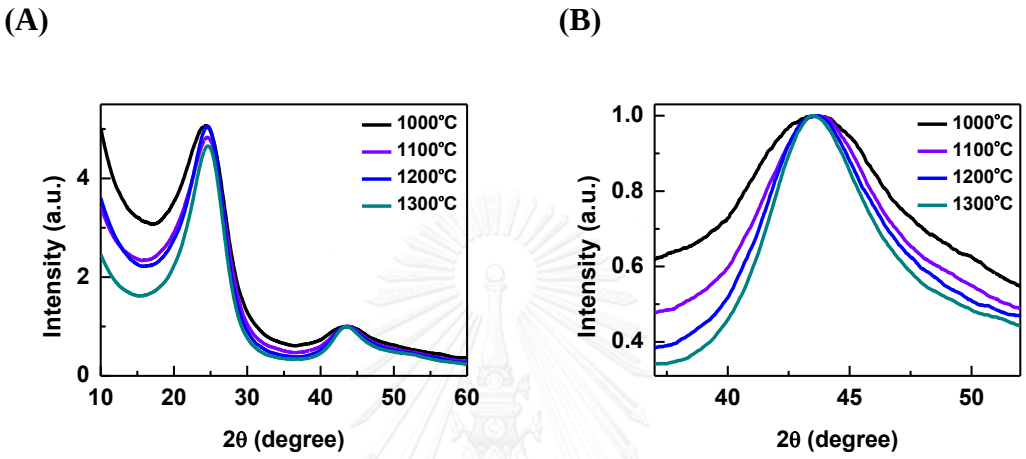

Fig. 4.9 (A) XRD pattern and (B) corresponding zoom-in XRD patterns for (10ℓ) plane of acetylene black synthesized at different temperatures (using an acetylene concentration of 10 %v/v and a residence time of 13.3 s).

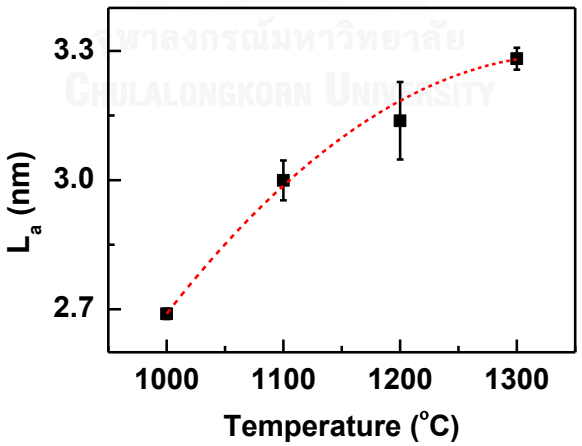

Fig. 4.10 Plot of L_a value calculated by Scherrer's equation against synthesis temperature (using an acetylene concentration of 10 %v/v and a residence time of 13.3 s).

To examine the band at 43.5° of (10ℓ) plane, Fig. 4.9 (B) shows the XRD pattern in the range from 34° to 53°. By using Scherrer's equation, an average crystal size in a-axis constantly increases from 2.689 ± 0.012 to 3.282 ± 0.025 nm when increasing synthesis temperature from 1000 to 1300 °C, as shown in Fig. 4.10.

Further chemical and crystal structure characterization were analyzed by Raman spectroscopy to obtain the molecular structure from specific vibration frequency and to predict the crystal size from vibrational defects in graphitic layers.

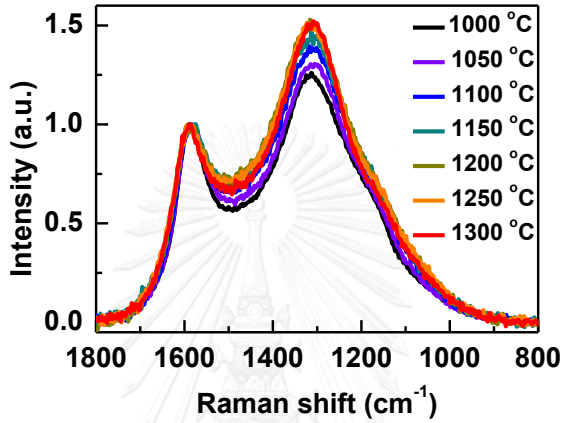

Fig. 4.11 Raman spectra of carbon black synthesized at different temperatures (using an acetylene concentration of 10 %v/v and a residence time of 13.3 s).

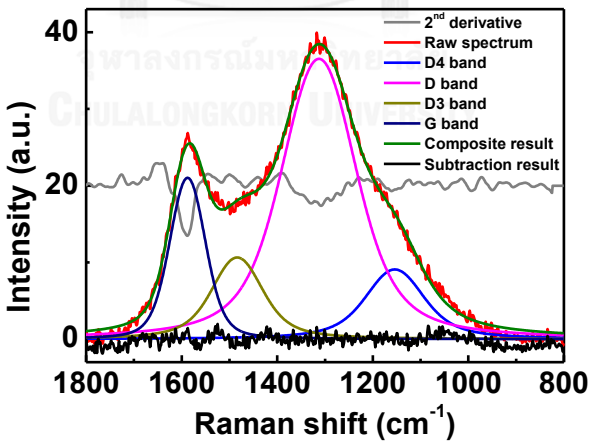

Fig. 4.12 Example of peak resolving Raman spectrum of acetylene black producing at 1200 ℃.

From Raman spectra in Fig. 4.11, two broad peak at 1590 and 1310 cm^{-1} are significantly observed. There have been several works reporting on Raman spectra of carbon. In numerous works of carbon, Raman peaks in the region of 1800–800 cm^{-1} compose of four important peaks. Thus, in this work, each Raman spectrum could be deconvoluted into four composite peaks, as shown in Fig. 4.12. A strong peak around 1590 cm^{-1} attributes to C=C

in-plane stretching lattice vibrations (E_{2g}) of the graphitic plane, which is so-called as "G (graphitic) band". Another strong peak around 1310 cm^{-1} attributes to defects inside the graphitic layer is D or D1 band. Two weak peaks around 1485 and 1165 cm^{-1} are D3 and D4 bands which relate defect carbon on interstitial places and sp^2 phase of transpolyacetylene, respectively [42]. Furthermore, band broadening of each peak is referred as strong disorder of graphite structure inside the particles. Raman peak assignments of carbon black are presented in Table 4.1.

Table 4.1 Raman peak assignments of acetylene black

Peak Position (cm^{-1})			Peak Assignments
Literatures	Perfect crystal	Current work	
1200–1140 (w)	-	1170–1145	D4 or I band: stretching vibrations of bond between sp^3 sites or sp^2 sites in polyene-like structures or ionic impurities [44]
1370–1300 (s)	-	1311–1324	D or D1 band: in plane stretching vibration mode between sp^2 site of conjugated form which activated by imperfect layer (A_{1g} symmetry) or graphitic lattice or edge of plane [44, 55]
1560–1468 (w)	-	1459–1491	D3, D", or A band: sp^3 vibration of amorphous carbon [43] on interstitial places (in plane defect) interfering the graphitic lattice of soot [44]
1610–1575 (s)	1575 (single crystal graphite) [46]	1582–1593	G band: in-plane breathing vibration mode between sp^2 sites of conjugated form (E_{2g} symmetry) [44, 56]

From Table 4.1, G band in this work was observed at 1580–1590 cm^{-1} which shifts from 1575 cm^{-1} of single crystal graphite or G band due to a decrease in crystal size or rise of defect on graphitic plane [46]. From G, D4, and D3 bands, it can be summarized that the molecular structure of acetylene black is a mixed form of the small graphitic structure, and the individual and interstitial amorphous structure.

Table 4.2 Raman intensity ratio after peak deconvolution at various temperatures

Temperature (°C)	Intensity ratio (%)			
	D4 (1170–1145 cm^{-1})	D (1311–1324 cm^{-1})	D3 (1459–1491 cm^{-1})	G (1582–1593 cm^{-1})
1000	11.035	45.384	11.612	31.970
1050	13.453	43.148	13.838	29.560
1100	13.724	43.540	14.550	28.187
1150	13.463	44.731	14.526	27.281
1200	14.885	43.398	15.652	26.065
1250	14.956	43.458	15.691	25.895
1300	13.299	45.186	15.773	25.742

Table 4.2 shows ratio of peak area in each peak composition (Fig. 4.12). Intensity ratio of D and G band (I_D/I_G) was used to calculate the mean crystal size in a-axis (L_a) by Ferrari's equation [37] which I_D/I_G directly correlates with the L_a value of graphitization degree over the range of high defect materials of graphitic structure. A number of studies used the inverse relevant between I_D/I_G and the L_a value which their crystals were high degree graphitization materials or related to large crystal size [45, 46, 48].

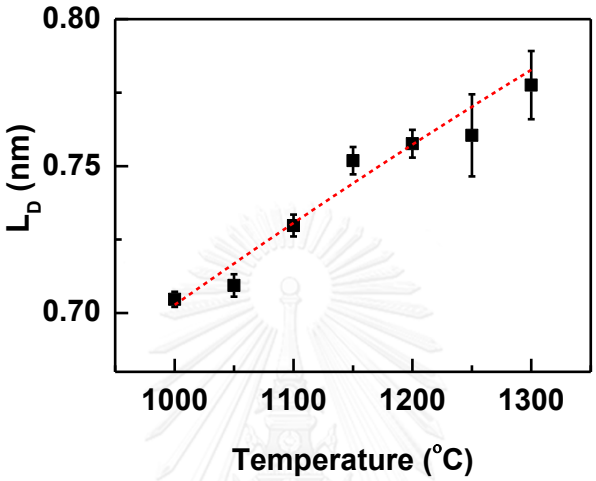

Fig. 4.13 Plot of L_D value calculated from Ferrari's equation against synthesis temperature (using an acetylene concentration of 10 %v/v and a residence time of 13.3 s).

Additional information, in Raman technique, the L_D (distance between defects of graphene plane; a-axis) calculation was generated from the graphene sample (not graphite-like structure) [37]. In this work, we used L_D as substituted L_a (crystal size in a-axis). From calculated L_D values at different synthesis temperatures (Fig. 4.13), L_D size of graphite like structure inside acetylene black particles has a strong tendency to increase from 0.705 ± 0.003 to 0.778 ± 0.012 nm with an increase in synthesis temperature from 1000 to 1300 °C**.** Even L_D and L_a values calculated from these two techniques of crystal measurements are not the same, this result is still good in agreement with the data from XRD analysis**.**

The results of XRD and Raman techniques are concluded that sizes of L_a are increased when increasing synthesis temperature because heat energy sinters the edges of adjacent micro-crystals to generate a larger size of crystal plane. Moreover, heat energy also drives the rate of pyrolysis and hydrogen-abstraction and carbon-addition reaction (HACA) [63]. HACA is the mechanism of PAHs formation which hydrogen atom is abstracted and carbon atom is added on a hydrocarbon molecule with radicals through pyrolysis reaction. This mechanism generates large L_a sizes or more complete crystals plane.

In the last part of temperature effect on chemical structure of acetylene black, it is focused on the chemical functional group. Acetylene black was analyzed by FT-IR microspectroscopy through the Ge ATR probe. On this acetylene black synthesis protocol, chemical functional group, *i.e.*, C–O and C=O in acetylene black should not be observed owing to process of pyrolysis reaction and non-oxidizing atmosphere.

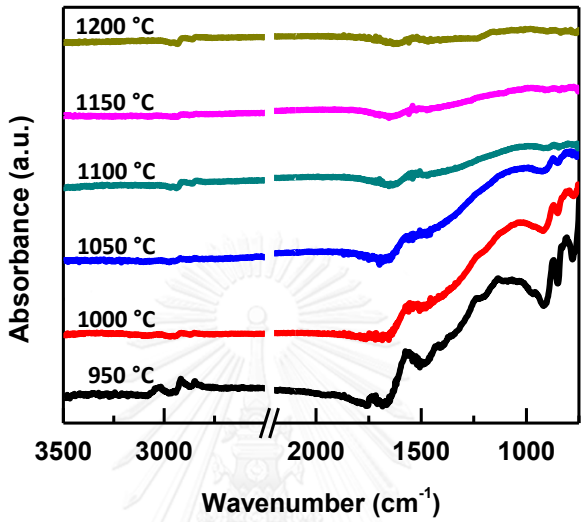

Fig. 4.14 IR spectra of acetylene black synthesized at various temperatures (using an acetylene concentration of 10 %v/v and a residence time of 13.3 s).

Fig. 4.14 shows IR spectra of acetylene black synthesized at different temperatures (950–1200 °C). At 950 °C, the absorption bands at 3016, 2917, 2848, 1417, 1360, 1235, 1136, 958, and 807–731 cm^{-1}, which are attributed to hydrocarbon residues on acetylene black product, are observed. In addition, the absorption band at 1575 cm^{-1} (in-plane stretching of C=C on graphitic structure with E_{1u} symmetry) and 871 cm^{-1} (out of plane displacement of C=C with A_{2u} symmetry) are characteristic of graphitic structure. According to IR results, synthesized acetylene black at low temperature is abundant of C–H groups and consists of saturated and unsaturated hydrocarbon and aromatic structure. These assignments are summarized in Table 4.3.

Table 4.3 Infrared peak assignments of acetylene black [36, 57-61]

Peak Position (cm^{-1})		Peak Assignments
Literatures	Current work	
3100–3000	3016 (2979–3072)	C—H stretching of unsaturated hydrocarbon
2930	2917 (2940–2878)	asymmetric C—H stretching of CH_2
2860	2848 (2867–2811)	symmetric C—H stretching of CH_2
~1700	1732 (1751–1684)	$=CH_2$ wagging vibration overtone
1600–1450, 1600 (s), 1587 (graphite)	1575 (1659–1484)	in-plane C=C stretching of aromatic with E_{1u} symmetry (graphitic structure)
1455–1435	1417 (1484–1406)	asymmetric C—H bending of aliphatic CH_3 or deformation of CH_2
1420–1350	1360 (1406–1338)	symmetric C—H bending of CH_3
1310–1260	1235 (1274–1203)	CH_2 twisting vibration of -(CH_2)-
1175–1165	1136/1068 (1203–976)	C—C stretching vibration or CH symmetric rocking vibration of alkene (CH in-plane vibration)
980–810	958 (976–920)	out of plane CH vibration
880–760	807 (801–835) 748 (776–714) 731 (776–714)	CH_2 out of plane blending of CH_2
867	871 (920–782)	out of plane displacement of C=C (A_{2u} symmetry)

Numerous works have characterized the functional groups of carbonaceous species by using FT-IR technique. The result of IR spectra in general hydrocarbon showed high intensity. IR spectra showed lower intensity and more baseline sloping when hydrocarbon had been transformed to carbon or synthesis temperature had been increased [61, 62]. As mentioned above, in these experiments, all peaks of IR spectra also entirely disappear when increasing synthesis temperatures. However, the graphitic structure which is generally active in IR spectra at 1600 cm^{-1} still remains and is confirmed by Raman results.

When temperature is increased, the drastic disappear of hydrocarbon structure, which decreases H component and increases C component in acetylene black, can be explained with HACA mechanism. From the IR results, the synthesis temperature of 1100 °C was likely suitable because of hydrocarbon peak disappearance, as shown in Fig. 4.14 after reaching such temperature. However, to confirm that hydrocarbon in carbon particle was totally changed to carbon, the synthesis temperature is set to 1200 °C for studying other parameters.

In addition, From Raman data (Fig. 4.11), amorphous carbon or sp^3 structure on interstitial place of graphitic lattice with C–H and C–C form are observed at any temperature.

Their results have not different. Otherwise, IR spectra of acetylene black produced over 1100 °C show the absence of C–H on carbon structure due to nonexistence of C–H vibration. It may be minimal amount until IR measurement cannot observed. It shows that the main chemical structure of acetylene black in form of amorphous is $sp^3$and disorder between carbon atom as major component.

4.1.3 Conclusions

For effect of temperature on morphology, heat energy induces a great number of nucleation at initial state and then decreases the primary particle size. Thus, the heat energy closely correlates to both aggregate size and surface area. However, heat energy does not affect the porosity of acetylene black because the reaction in this experiment does not consist of oxidizing agents which could removed carbon and generate pore in carbon particles [1, 19, 20]. For effect on chemical structure, the main structure of synthesized acetylene black composes of graphitic and amorphous structures. In both crystal analyses, Raman spectroscopy and XRD, being analogous technique, confirm that crystal size of graphitic like structure (L_a) goes larger because of the sintering between edges of graphitic plane and the heat-induced LPAH increment. Furthermore, the heat energy reduces the amount of hydrocarbon residue inside the acetylene black particle. These results inform that heat energy is a key factor to control the synthesis of acetylene black.

4.2 Effect of acetylene concentration on acetylene black synthesis

Acetylene black samples were prepared by varying acetylene concentration in the range of 10–70 %v/v. Acetylene gas was diluted with nitrogen gas when using a reactor temperature of 1200 °C and a residence time of 13.3 s to study the effect of concentration on acetylene black characters. After that, acetylene black was characterized with various technical analyses.

4.2.1 Effect of acetylene concentration on morphology of acetylene black

From SEM images (Fig. 4.15), the sizes of primary particle seem to be unchanged with an increase in acetylene concentration over the range of 10–70 %v/v. The particles size distribution and the average size of primary particles from acetylene black synthesized at various acetylene concentrations are presented in Fig. 4.16 and Fig. 4.17, respectively. They show that acetylene concentration does not affect the size of primary particle. The primary particles have their sizes in the range of 100 ± 16 to 109 ± 19 nm while the distributions are insignificantly changed.

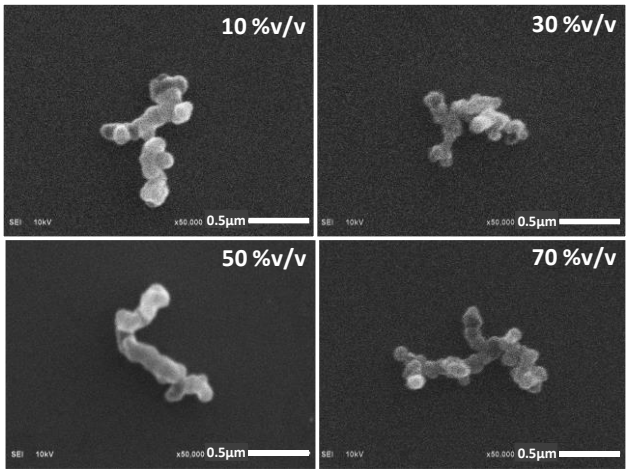

Fig. 4.15 SEM images of acetylene black synthesized at different acetylene concentrations (using a residence time of 13.3 s and a synthesis temperature of 1200 ℃).

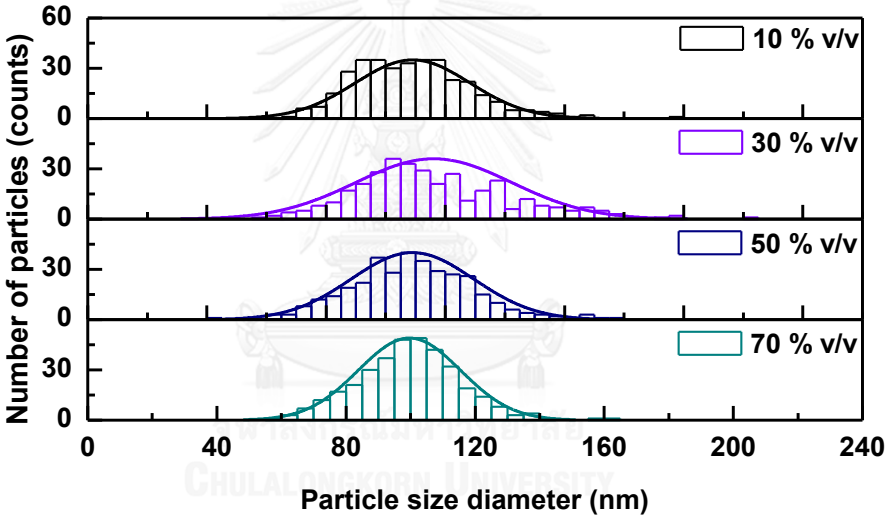

Fig. 4.16 Particles size distributions of primary particles of acetylene black synthesized at different acetylene concentrations (using a residence time of 13.3 s and a synthesis temperature of 1200 ℃).

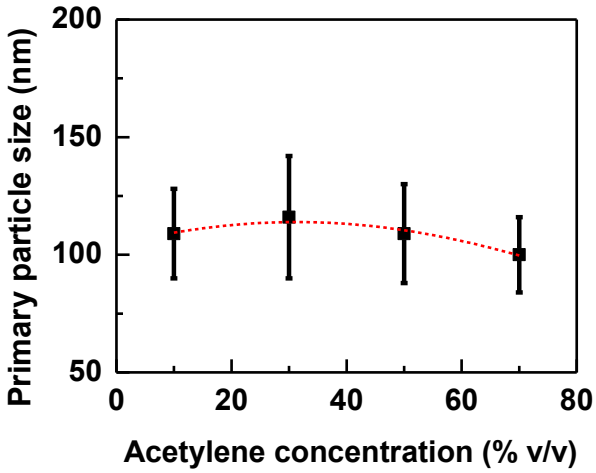

Fig. 4.17 Plot between primary particle size and acetylene concentration (using a residence time of 13.3 s and a synthesis temperature of 1200 ℃).

Owing to the indistinct information from the plot of primary particle size synthesized at 1200 °C. Acetylene black was additionally synthesized using various concentration at 1100 °C. SEM images and their average sizes of acetylene black at this condition are illustrated in Fig. 4.18 and Fig. 4.19.

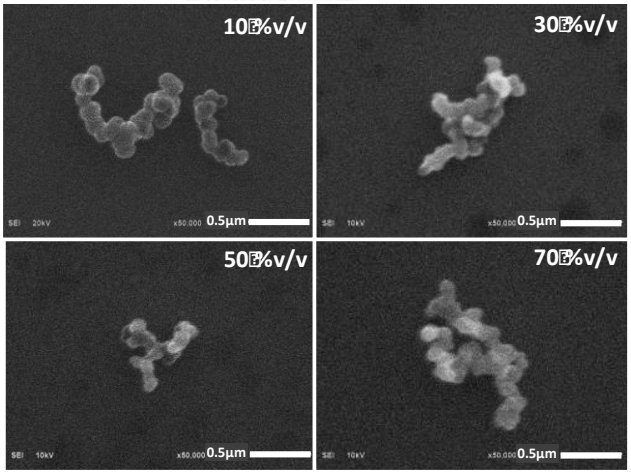

Fig. 4.18 SEM images of acetylene black synthesized at different acetylene concentrations (using a residence time of 13.3 s and a synthesis temperature of 1100 ℃).

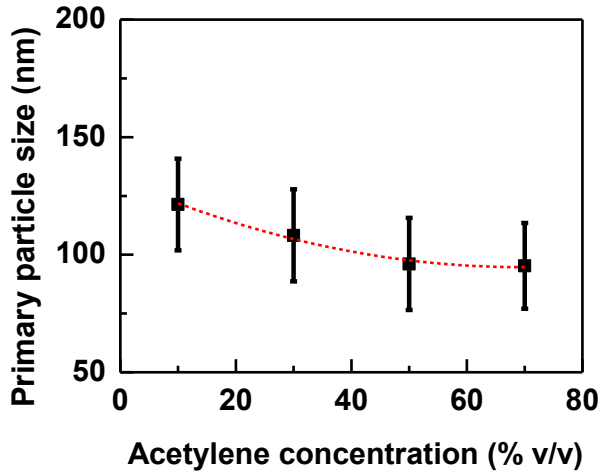

Fig. 4.19 Plot between primary particle size and acetylene concentration (using a residence time of 13.3 s and a synthesis temperature of 1100 ℃).

SEM images (Fig. 4.18) show that the size of primary particles is likely unchanged when increase in acetylene concentration at 1100 °C. Nevertheless, in Fig. 4.19, the measured primary particle size is decreased from 121 ± 19 to 96 ± 19 nm with an increase in acetylene concentration from 10 to 50 %v/v. After that, the primary particle size is slightly changed. This phenomena occurs at 1100 °C, but it does not occur at 1200 °C. As a result, the energy at 1200 °C may be sufficient to generate high LPAHs concentration for nucleation while SPAHs are small with the closed ratio at each concentration. On the other hand, energy at 1100 °C is insufficient. An increase in acetylene concentration rises the exothermic energy [64] and precursor concentration which drives LPAHs formation generating more carbon nuclei at the initial step whereas reduces SPAHs formation growing particle size in the next step. For this reason, when acetylene concentration is increased, primary particle size is decreased. However, this result is irrelevant to Ono's study which presented a small increase in primary particle size from 42 to 52 nm with an increase in acetylene concentration using of low concentrations of acetylene (between 0–5 vol%) when mixing with 1 vol% of benzene at 1200 °C [7]. Nevertheless, the range of synthesized concentration of Ono's study did not cover this work.

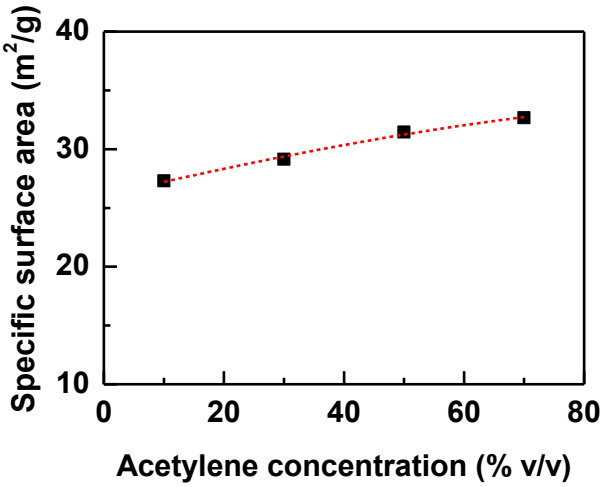

Fig. 4.20 Plot of specific surface area against acetylene concentration (using a residence time of 13.3 s and a synthesis temperature of 1200 ℃).

The surface area of acetylene black synthesized using various acetylene concentrations at 1200 °C is shown in Fig. 4.20. When increasing acetylene concentration from 10 to 70 %v/v, specific surface area is slightly increased from 27.296 to 32.662 m^2/g. These results can infer that size of primary particle at different acetylene concentration at 1200 °C may be decreased. Because all synthesized acetylene black samples are non-porous structure, their specific surface area directly relates to the primary particle size of all samples. Therefore, higher temperature conditions just reduce the difference in acetylene concentration effect on primary particle size and surface area of acetylene black.

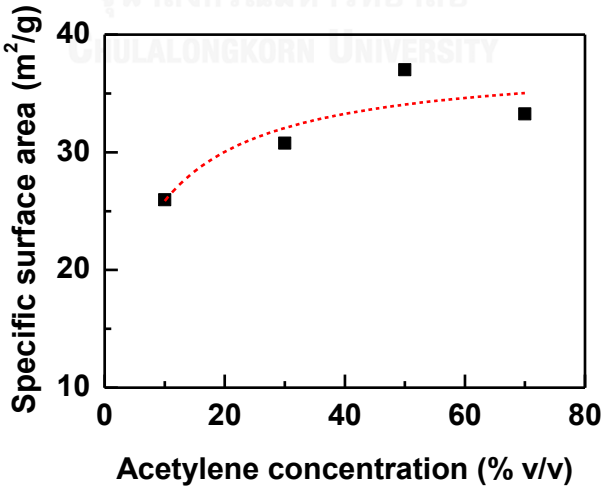

Fig. 4.21 Plot of specific surface area against acetylene concentration (using a residence time of 13.3 s and a synthesis temperature of 1100 ℃).

The specific surface area of acetylene black synthesized at 1100 °C using various acetylene concentrations are also determined and displayed in Fig. 4.21. The result shows that surface area is increased from 25.970 to 37.265 m^2/g with an increase in acetylene concentration from 10 to 50 %v/v. These results are also the relative of the specific surface area and primary particle as the result at 1200 °C. The specific surface area is increased, whereupon sizes of primary particle is decreased. This result of surface characterization is related to the results from Tesner's study revealing that surface area was increased with an increase in feed stock concentration between 0–8 % of benzene (precursor) and 0–20 % of acetylene (precursor) mixing with methane at 1300 °C by using different instrument construction [65]. Nevertheless, it does not agreed with the pervious group study about soot formation during acetylene pyrolysis [66], which surface area of soot particle was decreased from 55 to 30 m^2/g when increasing acetylene concentration from 3 to 25 % at 1300 °C with 5 times shorter furnace tube and helium gas as mobile phase. However, this work used high range of acetylene concentration which were significantly larger than the previous works.

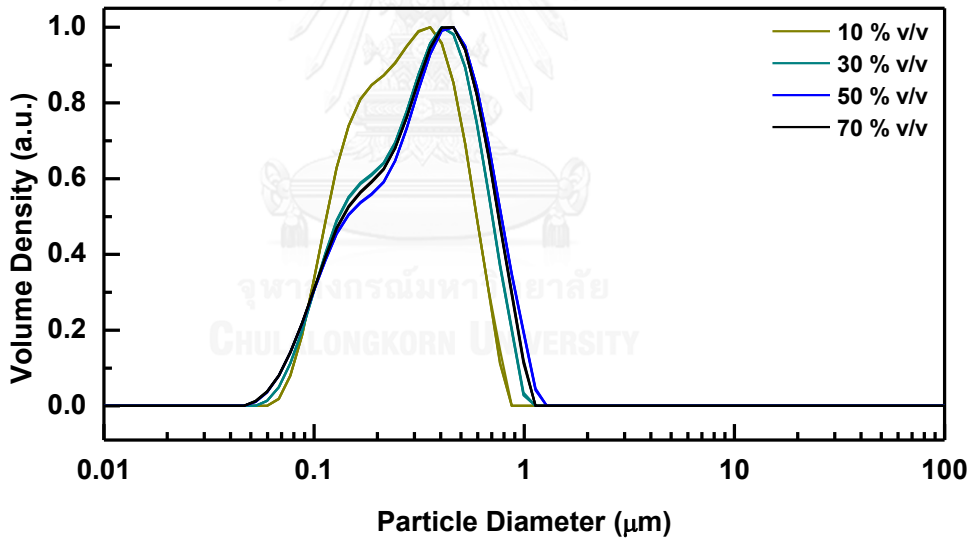

Fig. 4.22 Particles size distributions of acetylene black synthesized at different acetylene concentrations (using a residence time of 13.3 s and a synthesis temperature of 1200 ℃).

Only SEM images in Fig. 4.15 cannot be used to determine the aggregate size of synthesized acetylene black exactly. Their external morphology seems still similar. To confirm the effect of acetylene concentration on aggregate size, acetylene black was characterized by DLS technique, as shown in Fig. 4.22.

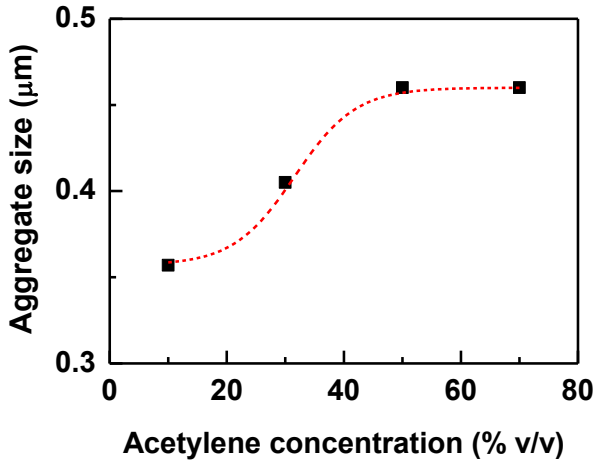

Fig. 4.23 Plot between aggregate size of acetylene black and acetylene concentration (using a residence time of 13.3 s and a synthesis temperature of 1200 ℃).

Fig. 4.23 shows the relation of acetylene concentration and aggregate size of acetylene black synthesized at 1200 °C. Their size is increased from 0.357 to 0.460 μm when increasing acetylene concentration from 10 to 50 % v/v and invariable after 50 % v/v. It seems that acetylene concentration affects the aggregate size directly since high concentration of feed stock (acetylene) promotes the primary particle aggregation [1].

4.2.2 Effect of acetylene concentration on chemical structure of acetylene black

From XRD pattern on Fig. 4.24 (A), in the case where there was a change of acetylene concentration between 10–70 % v/v at 1200 °C, no change in peak position and peak distribution are observed for each acetylene concentration. Nevertheless, the peaks are expanded for observing more details in Fig. 4.24 (B). To deeply examine, FWHM and peak position of (10ℓ) plane are determined for calculated the L_a size using Scherrer's equation.

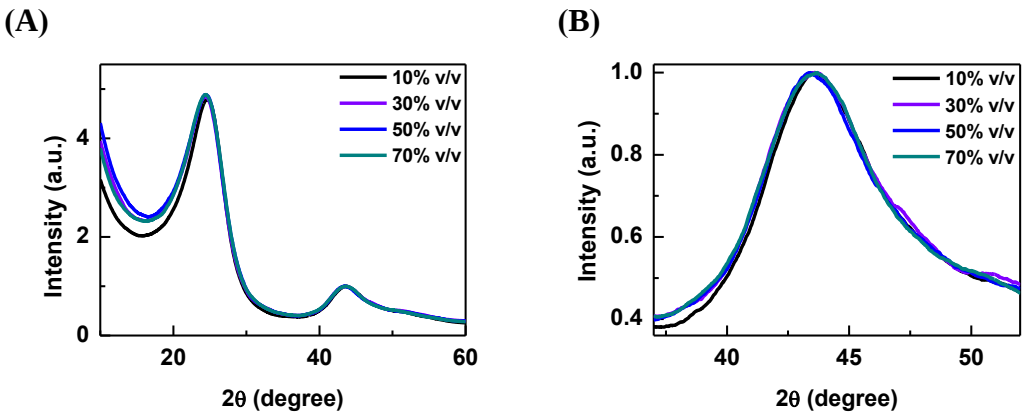

Fig. 4.24 (A) XRD pattern and (B) corresponding zoom-in XRD patterns for (10ℓ) plane of acetylene black synthesized at different acetylene concentrations (using a residence time of 13.3 s and a synthesis temperature of 1200 ℃).

L_a sizes of micro-crystals calculated from (10ℓ) plane of XRD pattern using Scherrer's equation are shown in Fig. 4.25. The mean values of L_a are insignificantly increase from 3.138 ± 0.090 and 3.199 ± 0.083 nm with an increase in acetylene concentration from 10 to 70 %v/v.

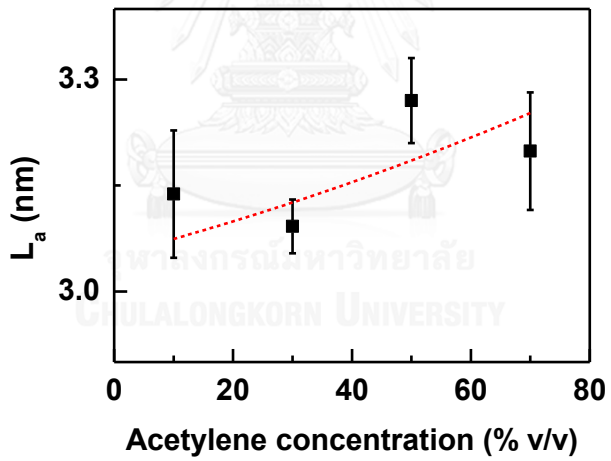

Fig. 4.25 Plot of L_a value calculated by Scherrer's equation against acetylene concentration (using a residence time of 13.3 s and a synthesis temperature of 1200 ℃).

Raman spectra of acetylene black synthesized at 1200 °C using various acetylene concentration are shown in Fig. 4.26. Their spectra are deconvoluted to separate peak compositions for further analysis. Peak characters of Raman spectra and the intensity ratio of all peak compositions are shown in Table 4.1 and Table 4.4, respectively.

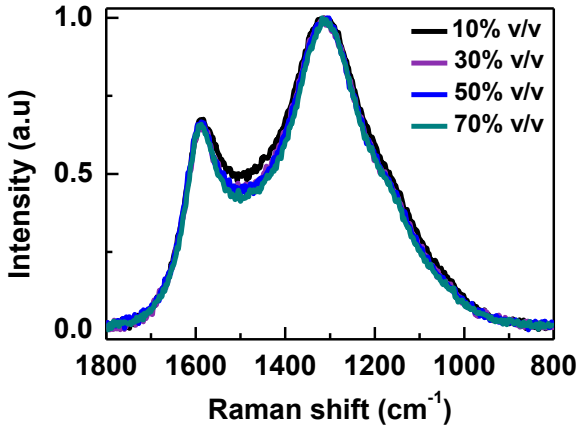

Fig. 4.26 Raman spectra of carbon black synthesized at different acetylene concentrations (using a residence time of 13.3 s and a synthesis temperature of 1200 ℃).

Table 4.4 Raman intensity ratio after peak deconvolution at various acetylene concentrations

Acetylene concentration (%v/v)	Intensity ratio (%)			
	D4 (1170–1145 cm^{-1})	D (1311–1324 cm^{-1})	D3 (1459–1491 cm^{-1})	G (1582–1593 cm^{-1})
10	14.885	43.398	15.652	26.065
30	13.718	45.088	14.766	26.428
50	15.025	43.728	15.524	25.724
70	12.442	47.030	13.544	26.984

The ratio of G and D band intensities from Table 4.4 was used to calculate the L_D value by Ferrari's equation, as shown on Fig. 4.27. The crystal sizes is slightly increased in the range of 0.758 ± 0.005 to 0.775 ± 0.004 nm with increase in acetylene concentration. This provides the evidence for the fact that acetylene concentration slightly affects the crystal generating, which is in good agreement with XRD results.

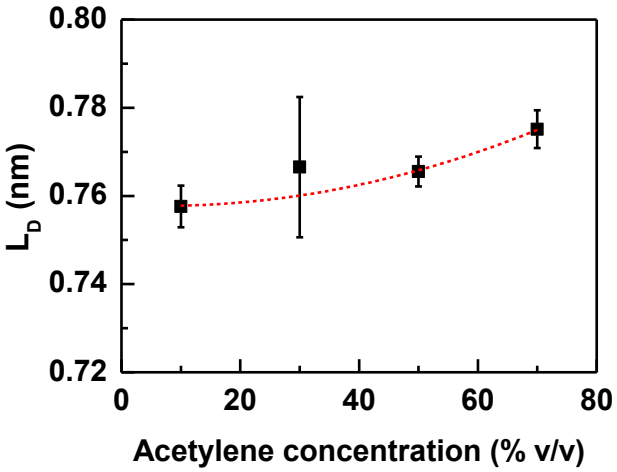

Fig. 4.27 Plot of L_D value calculated from Ferrari's equation against acetylene concentration (using a residence time of 13.3 s and a synthesis temperature of 1200 ℃).

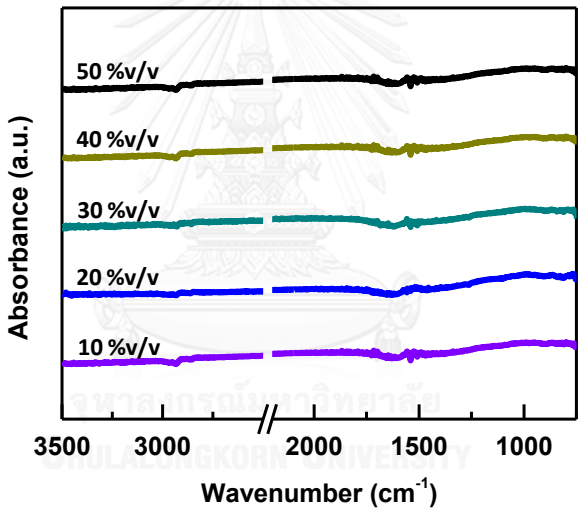

Fig. 4.28 IR spectra of acetylene black synthesized at various acetylene concentrations (using a residence time of 13.3 s and a synthesis temperature of 1200 ℃).

From IR spectra (Fig. 4.28) of acetylene black synthesize at various acetylene concentration, 1200 °C, and 13.3 s reaction time, no peak character of any fuctional group are observed. This resuIt implies that if heat energy is high enough as 1200 °C, all hydrogen atom in precursor will be totally eliminated from carbon particles (even the concentration of carbon precursor is increased).

4.2.3 Conclusions

An increase in acetylene concentration drives saturated system of precursor at the initial state of acetylene black synthesis and may increase the heat energy by exothermic

reaction of acetylene out of the receving energy from electrical furnace. The primary particles are smaller togerther with an increase in surface area (relative character: nonporosity material). Likewise, this phenomenon induces the collision between the primary particle with more saturating system of particles at the initial state, then unit size of aggregate particle are larger. This may induce the collision between molecules, which slightly increase the size of graphite like structure. However, an increase in concentration do not push the system to get more organic residue in their structure from incomplete convertion which is affected by high concentration of precursor at the same input energy (furnace temperature).

4.3 Effect of residence time on acetylene black synthesis

Residence time of acetylene gas (carbon precursor) inside the reactor was altered by controlling flow rate of total feedstock. This parameter is very important for numerous studies [7, 49, 52] because it relates to the reaction time, growing time, and collision range of carbon particles while the reaction is continued.

4.3.1 Effect of residence time on morphology of acetylene black

SEM images in Fig. 4.29 show the morphology of aggregate structure and primary particle of acetylene black synthesized by using different residence times of feedstock. When varying the residence time between 3.5–22.2 s, a change in external morphology of acetylene black is not observed.

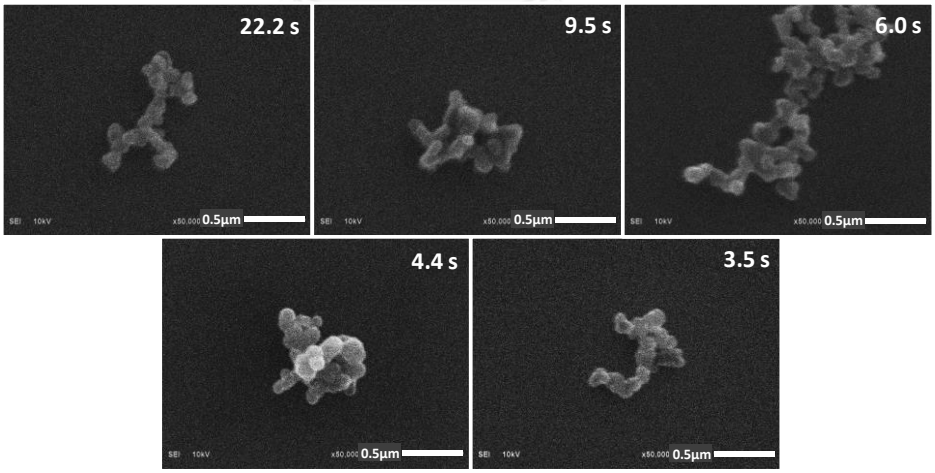

Fig. 4.29 SEM images of acetylene black synthesized at different residence times (using an acetylene concentration of 10 %v/v and a synthesis temperature of 1200℃).

Fig. 4.30 and Fig. 4.31 show the particle size distribution and plot of mean primary particle size at various residence times. Primary particle size of acetylene black is increased from 101 ± 20 nm to 121 ± 20 nm while the residence time of feed stock in the reactor is increased from 3.5 until 22.2 s. It can be explained that, at fixed temperature, free generated

SPAHs in reaction system continuously deposit on the surface of particle [7]. A short residence time provides a short period for surface growth by that deposition. It leads to small primary particles.

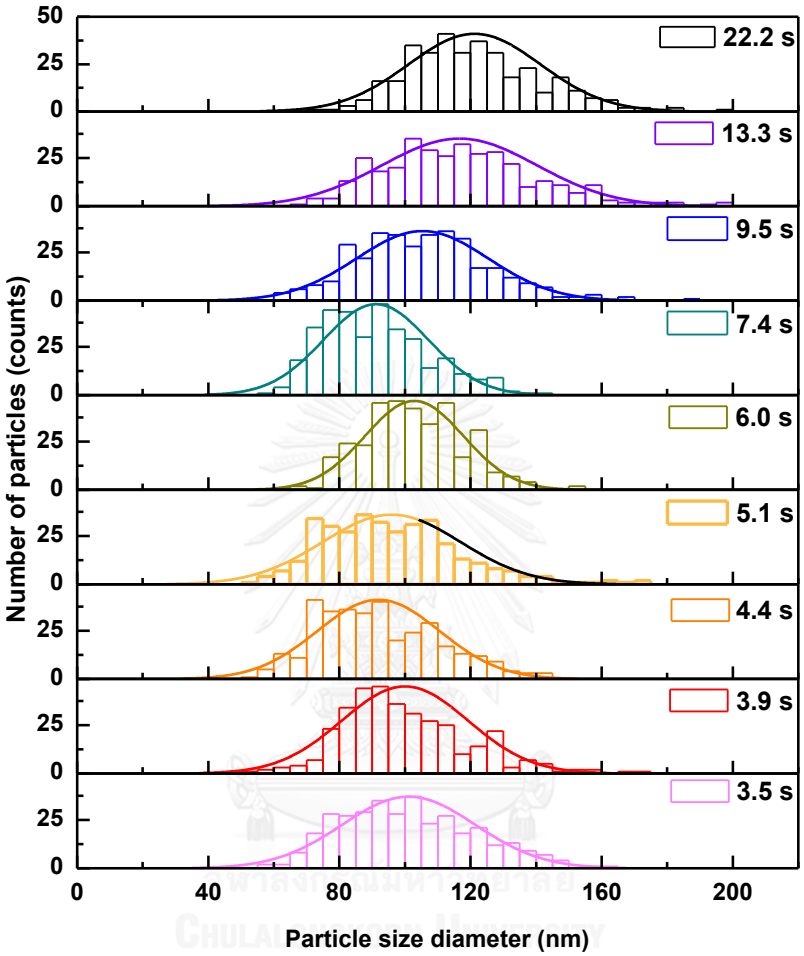

Fig. 4.30 Particles size distributions of primary particles of acetylene black synthesized at different residence times (using an acetylene concentration of 10 %v/v and a synthesis temperature of 1200℃).

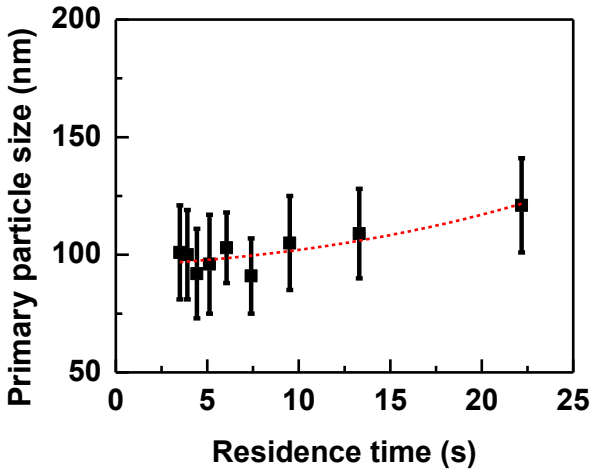

Fig. 4.31 Plot between primary particle size and residence time (using an acetylene concentration of 10 %v/v and a synthesis temperature of 1200℃).

By varying residence times over the range of 3.5–22.2 s at 1100 °C with 10 %v/v acetylene gas, the primary particle sizes are constant around 120 ± 17 to 127 ± 22 nm, as shown in Fig. 4.32 and Fig. 4.33. The residence time insignificantly affects on the growth mechanism at 1100 °C synthesized temperature. This result is different from the SEM data of varying concentration at 1200 °C. By decreasing synthesis temperature to 1100 °C, the sizes of primary particle diameter are larger with lower surface energy. The rate of surface growth are decreased. Therefore, primary particle size is not significantly increased with an increase in recidence time (growing time) at low temperature as 1100 °C.

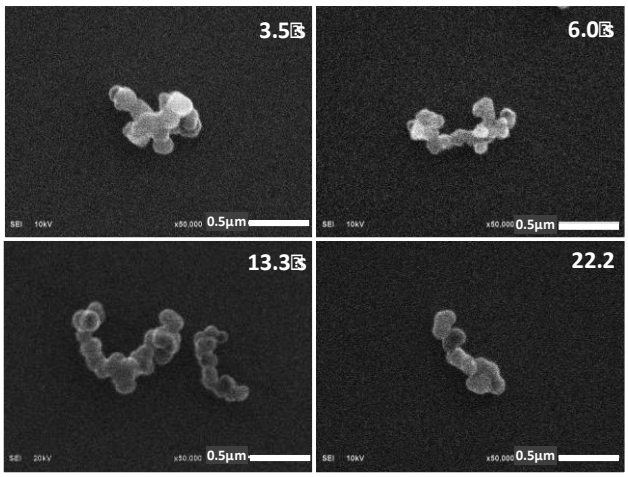

Fig. 4.32 SEM images of acetylene black synthesized at different residence times (using an acetylene concentration of 10 %v/v and a synthesis temperature of 1100℃).

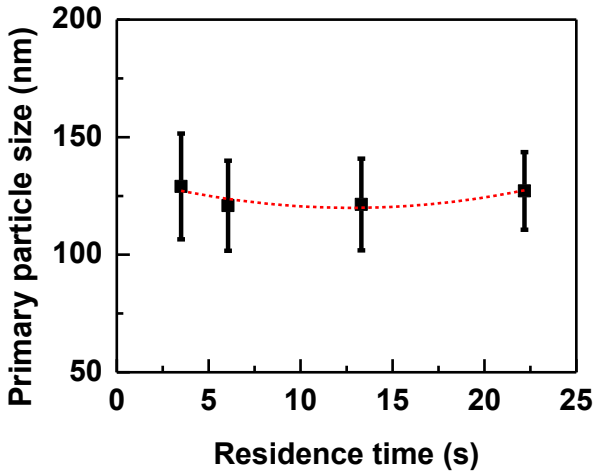

Fig. 4.33 Plot between primary particle size and residence time (using an acetylene concentration of 10 %v/v and a synthesis temperature of 1100℃).

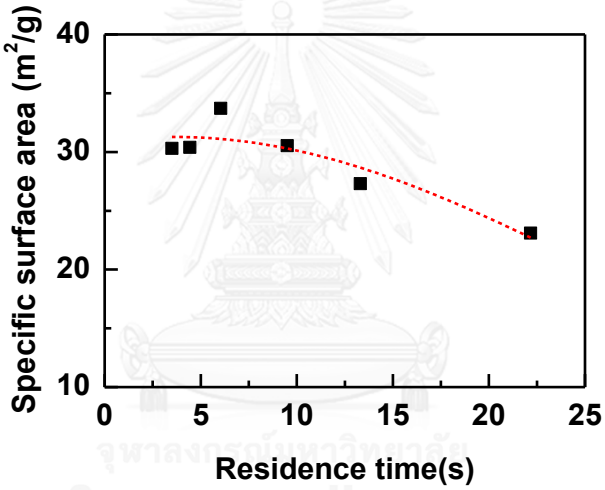

Fig. 4.34 Plot of specific surface area against residence time (using an acetylene concentration of 10 %v/v and a synthesis temperature of 1200℃).

In the case of specific surface area, the specific surface area is increased from 23.091 to 33.709 m^2/g when residence time is reduced from 22.2 to 6.0 s at 1200 °C. For shorter residence times than 6.0 s, the specific surface area is approximately 30.389 m^2/g, as shown in the graph of specific surface area at different residence times (Fig. 4.34). To describe this observation, the results are compared to the trend of primary particle size with the same synthesis conditions. It implies that surface area is also actually based on the primary particle size.

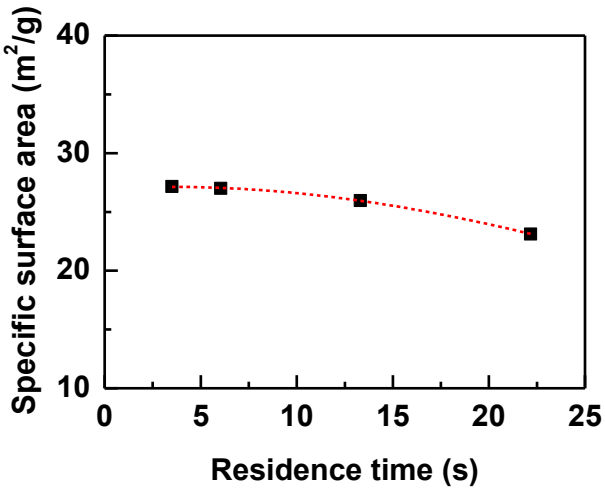

Fig. 4.35 Plot of specific surface area against residence time (using an acetylene concentration of 10 %v/v and a synthesis temperature of 1100℃).

Fig. 4.35 shows the plot of a specific surface area of acetylene black produced by various residence times at the synthesized temperature of 1100 °C, their sizes are slightly decreased from 27.001 to 23.123 m^2/g with increase in residence time from 6.0 to 22.2 s. This result also relates to the primary particle size which are reduced by growing time of particles (a decrease in residence time in the synthesis using 10 %v/v of acetylene at 1100 °C).

SEM images in Fig. 4.29 show external aggregate morphology of acetylene black synthesized by different residence times between 3.5 to 22.2 s. The sizes of aggregate particles were measured by DLS technique and their most population values are plotted against the residence times, as shown in Fig. 4.36 and Fig. 4.37, respectively. The results show that the most population sizes of aggregate structures are fluctuated. However, the trend shows an increase in the aggregate size in the range of 0.214–0.405 μm. In the studies of soot aggregation, carbon black or soot generation was used to illustrate the effect of residence time on the aggregate sizes. A longer residence time increases the time of collision between primary or group of particles [67]; therefore, aggregate particle size tends to be larger.

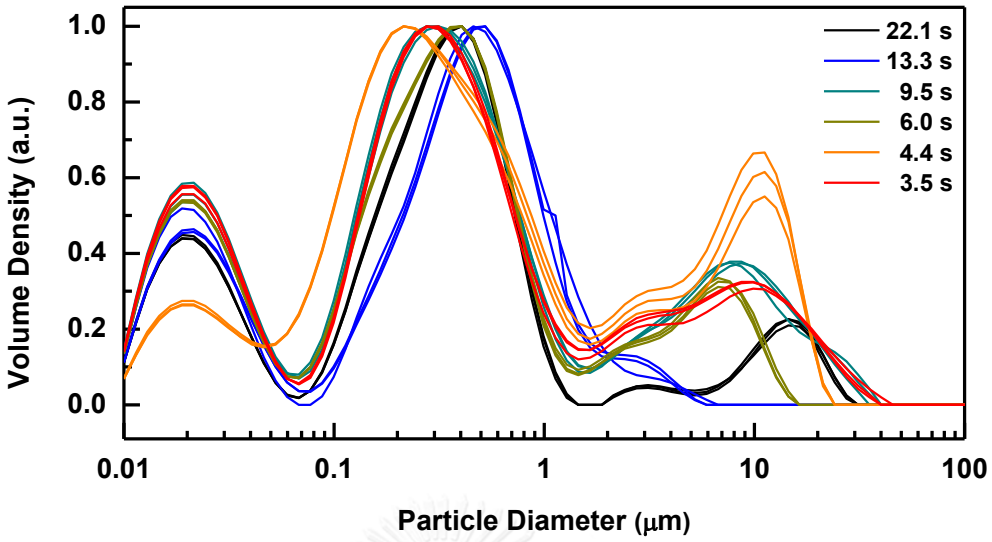

Fig. 4.36 Particles size distributions of acetylene black synthesized at different residence times (using an acetylene concentration of 10 %v/v and a synthesis temperature of 1200℃).

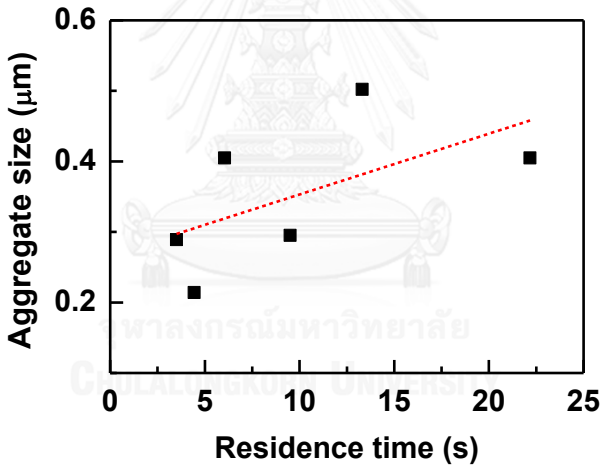

Fig. 4.37 Plot between aggregate size of acetylene black and residence time (using an acetylene concentration of 10 %v/v and a synthesis temperature of 1200℃).

4.3.2 Effect of residence time on chemical structure of acetylene black

The effect of residence time on crystal structure was elucidated from XRD patterns in Fig. 4.38. Especially focusing on (10ℓ) plane, band width of this peak seems to be sharper with an increase in a residence time. To get the explicit results from XRD data, FWHM of (10ℓ) plane was measured and the mean L_a value was calculated by Scherrer's equation, as shown in the Fig. 4.39. Mean sizes of L_a are slightly increased from 2.948 ± 0.067 nm to 3.160 ± 0.058 nm with an increase in residence time.

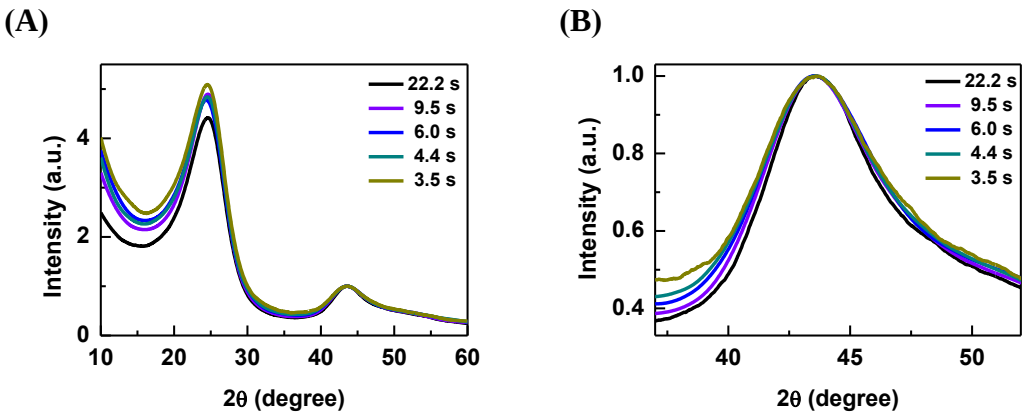

Fig. 4.38 (A) XRD pattern and (B) corresponding zoom-in XRD patterns for (10ℓ) plane of acetylene black synthesized at different residence times (using an acetylene concentration of 10 %v/v and a synthesis temperature of 1200 ℃).

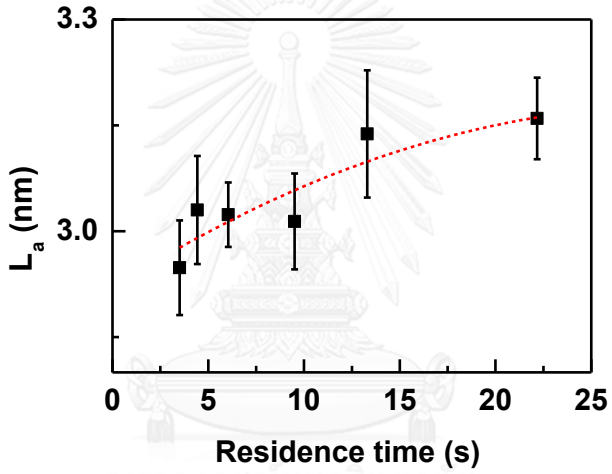

Fig. 4.39 Plot of L_a value calculated by Scherrer's equation against residence time (using an acetylene concentration of 10 %v/v and a synthesis temperature of 1200 ℃).

Fig. 4.40 shows Raman spectra of acetylene black synthesized using different residence times. The observed spectra are an indifferent in component peaks. All peak characters of Raman spectra are shown in Table 4. 1. Peak shapes and positions are similar at various residence times. Raman spectra was deconvoluted to show the exact characters. The ratio of each band is shown in Table 4.5.

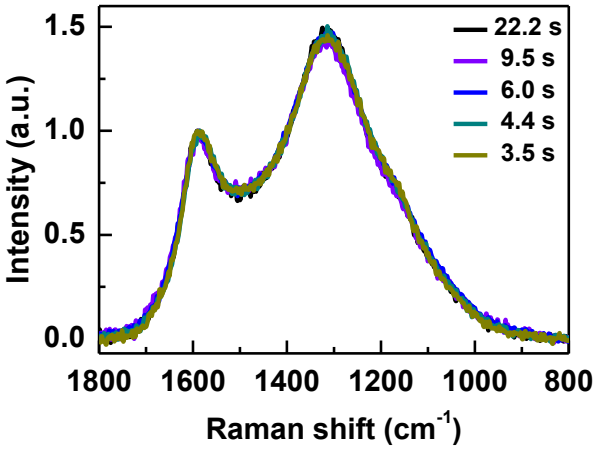

Fig. 4.40 Raman spectra of carbon black synthesized at different residence times (using an acetylene concentration of 10 %v/v and a synthesis temperature of 1200 ℃).

Table 4.5 Raman intensity ratio after peak deconvolution at various residence times

Residence time (s)	Intensity ratio (%)			
	D4 (1170–1145 cm^{-1})	D (1311–1324 cm^{-1})	D3 (1459–1491 cm^{-1})	G (1582–1593 cm^{-1})
3.5	14.552	45.361	12.282	27.806
4.4	13.427	45.638	13.870	27.064
6.0	15.866	42.311	15.797	26.026
9.5	15.196	43.627	14.918	26.259
22.2	13.774	45.271	15.138	25.817

By using Ferrari's equation for calculating the L_D values from I_D/I_G ratio, the L_D sizes obtained from different residence times are plotted in Fig. 4.41. Relative short residence time generates the carbon particles with L_D size of 0.750 ± 0.005 nm, but for a longer residence times (up to 22.2 s), the L_D size is slightly increased to 0.777 ± 0.010 nm. From both analysis data as mentioned above, the crystal size is increased with longer residence time. It contributes to the sintering between edges of crystal plane, which occurs more sintering in the reaction zone. Therefore, longer residence time provides longer time of carbon particles in the reaction zone for that sintering to growth a larger L_D.

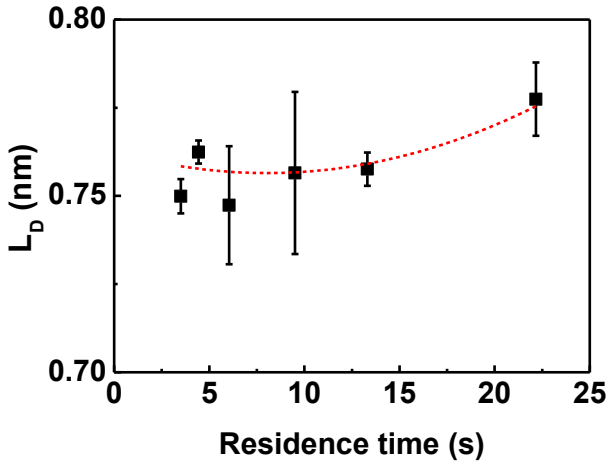

Fig. 4.41 Plot of L_D value calculated from Ferrari's equation against residence time (using an acetylene concentration of 10 %v/v and a synthesis temperature of 1200℃).

The residence time of feedstock was varied from 8.3–19.0 s to study the chemical structure of acetylene black which was analyzed by FT-IR spectroscopy, as shown in Fig. 4.42. From the results, residence time of carbon does not affect the chemical functional groups that are active in IR mode due to the complete thermal decomposition reaction at the synthesized temperature of 1200 °C.

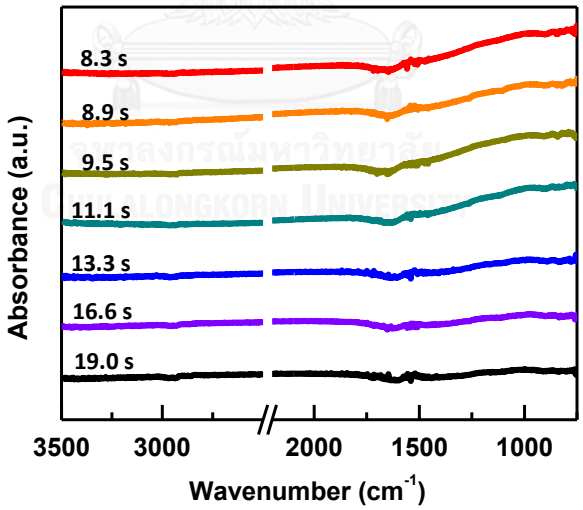

Fig. 4.42 IR spectra of acetylene black synthesized at various residence times (using an acetylene concentration of 10 %v/v and a synthesis temperature of 1200℃).

4.3.3 Conclusions

From the theory of carbon particle generating, in an initiation step, nuclei are generated and formed the first particle in a very short time. Such particle is grown continuously after. Increasing residence time of feed stock is similar to rising the time of particle growth rather

nucleation. Longer growth region generally increases the growth of primary particle size from free hydrocarbon residues and relates to a decrease in their surface areas being nonporosity material from all isotherm. Moreover, surface area property relates to the sintering effect within the aggregate particle which decreases the neck and gaps (surface area) between primary particles when increase in residence time. Furthermore, with long residence time, the aggregate size is increased by the effect of collision and sintering between aggregate particles. On the other hand, extending the time of growth induces the sintering between the edge of graphitic-like structure. The size of crystal tends to be larger. Due to sufficient energy condition of acetylene black synthesized at 1200 °C, hydrocarbon is totally converted to carbon materials. A change in chemical structure cannot observe by IR spectroscopy.

Table 4.6 The result of effect of synthesis parameters on acetylene black characters

Parameter	ΔPrimary particle size (nm)	ΔSurface area (m^2/g)	ΔAggregate particle size (nm)	ΔL_a (nm)	ΔL_D (nm)
↑ Temperature	-67	+14.540	-0.923	+0.593	+0.073
↑ Acetylene concentration (at 1100 °C)	-25	+11.295	+0.103	+0.061	+0.017
↑ Residence time (at 1200 °C)	+20	-10.618	+0.191	+0.212	+0.027

Remarks: + increase

- decrease

To conclude the results from three parameters, Table 4.6 shows the changing values of each character of acetylene black to analysis from their distinctions.

Firstly, parameter of temperature mostly changes the acetylene black characters by decrease in primary particle size for 67 nm, and aggregate particle size for 0.923 nm, and increase in surface area for 14.540 m^2/g, L_a size for 0.593 nm and L_D size for 0.073 nm.

Secondly, parameter of residence time appropriately increases in primary particle size for 20 nm, aggregate size for 0.191 nm, L_a for 0.212 nm and L_D for 0.027 nm, and decreases in surface area for 10.618 m^2/g.

Finally, the lowest effect of parameter is from acetylene concentration by decrease in primary particle size for 25 nm and increase in surface area for 11.295 m^2/g.

CHAPTER V

CONCLUSIONS

In this work, basic parameters for acetylene black synthesis, *i.e.*, temperature (heat generating), feedstock concentration (acetylene gas as a precursor and nitrogen gas as a diluent), and residence time (a total flow rate of feed stock) are studied to investigate morphological and chemical structure changes of synthesized carbon black without pre- or post-treatment.

Temperature (heat from electrical furnace) is an essential energy source for synthesizing carbon black in acetylene black process. It is the highest effective parameter compared with others because the temperature is important for all reactions in a whole system, including the generation of LPAHs (a key of nucleation at an initial step). Increasing reactor temperature in the range of 1000–1300 °C, primary particle and aggregate size are decreased to 67 nm and 0.923 μm, respectively, while specific surface area is increased for approximately 14.540 m^2/g. Because the temperature promotes the LPAHs formation which contributes to a great number of nucleation at an initial state and reduces the SPAHs which play a major role in the terminal part of a growing step. On the chemical structure of acetylene black, the size of crystal is larger at higher by the sintering effect. The chemical functional group of organic hydrocarbon is decreased and disappeared with an increase in temperature over 1100 °C.

For chemical structure of acetylene black, both of acetylene concentration and residence time very slightly affect to increase the crystal size (atomic regulation) with the reasons of molecular collision energy and sintering time, respectively. Moreover, the results of both parameters on functional groups cannot observed because the synthesis temperature is high enough to eliminate all IR-active functional group from carbon structure.

For morphological structure of acetylene black, higher concentration of precursor provides higher reaction energy which creates more nucleation, more collision probability between molecules (nucleation) and particles (aggregate formation), and more energy for nucleation and sintering. Almost all effects of acetylene concentration on acetylene black character is similar to the effect of temperature with the same reason of more nucleation and reaction energy. One different effect is the aggregate size which increases in size due to high collision of individual particles when acetylene concentration is increased.

However, effect of residence time contrasts with that of temperature parameter on morphological aspect of acetylene black due to emphasis on the growth step (reaction time of SPAHs and particle collision is a key). Increasing residence time increases the primary particle size, aggregate size, and crystal size by the reason of longer reaction time.

Although residence time and acetylene concentration just slightly affect the character of synthesized acetylene black, all parameters are completely investigated to provide potential information for controlling acetylene black synthesis in difference way to get the expected properties of acetylene black.

REFERENCES

1. Donnet, J.-B., B.R. Chand, and M.J. Wang, *Carbon black: science and technology*. 2 ed. 1993: MARCEL DEKKER, INC. 461.
2. Katz, M.J., *Some adsorption data on acetylene black.* J. Phys. Chem., 1956. **60**(9): p. 1338-1339.
3. Giet, C., *Acetylene black with high electrical conductivity and high absorptive power*. 1981, Produits Chimiques Ugine Kuhlmann, Courbevoie, France.
4. Orbach, H.K., *Production of carbon black*. 1963, Ashland Oil Inc.
5. Bolouri, K.S. and J. Amouroux, *Reactor design and energy concepts for a plasma process of acetylene black production.* Plasma Chem. Plasma P., 1986. **6**(4): p. 335-348.
6. Mendiara, T., et al., *An experimental study of the soot formed in the pyrolysis of acetylene.* J. Anal. Appl. Pyrol., 2005. **74**(1–2): p. 486-493.
7. Ono, K., et al., *Effect of benzene–acetylene compositions on carbon black configurations produced by benzene pyrolysis.* Chem. Eng. J., 2013. **215–216**: p. 128-135.
8. Inagaki, M. and F. Kang, *Fundamental science of carbon materials*, in *Materials Science and Engineering of Carbon: Fundamentals (Second Edition)*. 2014, Butterworth-Heinemann: Oxford. p. 17-217.
9. Ren, Z., Y. Lan, and Y. Wang, *Introduction to carbon*, in *Aligned Carbon Nanotubes.* 2013, Springer-Verlag Berlin Heidelberg. p. 1-5.
10. Donnet, J.-B., *Fifty years of research and progress on carbon black.* Carbon, 1994. **32**(7): p. 1305-1310.
11. Clague, A.D.H., et al., *A comparison of diesel engine soot with carbon black.* Carbon, 1999. **37**(10): p. 1553-1565.
12. Long, C.M., M.A. Nascarella, and P.A. Valberg, *Carbon black vs. black carbon and other airborne materials containing elemental carbon: Physical and chemical distinctions.* Environ. Pollut., 2013. **181**: p. 271-286.
13. Lahaye, J., G. Prado, and J.B. Donnet, *Nucleation and growth of carbon black particles during thermal decomposition of benzene.* Carbon, 1974. **12**(1): p. 27-35.
14. Siegmann, K., K. Sattler, and H.C. Siegmann, *Clustering at high temperatures: carbon formation in combustion.* J. Electron. Spectrosc. Relat. Phenom., 2002. **126**(1–3): p. 191-202.

15. Richter, H. and J.B. Howard, *Formation of polycyclic aromatic hydrocarbons and their growth to soot—a review of chemical reaction pathways.* Prog. Energy Combust. Sci., 2000. **26**(4–6): p. 565-608.

16. Lahaye, J. and F. Ehrburger-Dolle, *Mechanisms of carbon black formation. Correlation with the morphology of aggregates.* Carbon, 1994. **32**(7): p. 1319-1324.

17. Wojtoniszak, M. and E. Mijowska, *Controlled oxidation of graphite to graphene oxide with novel oxidants in a bulk scale.* J. Nanopart. Res., 2012. **14**(11): p. 1248.

18. Kinoshita, K., *Carbons*, in *Handbook of Battery Materials*, C. Daniel and J.O. Besenhard, Editors. 2011, Wiley-VCH Verlag GmbH & Co. KGaA. p. 269-284.

19. Schröder, A., M. Klüppel, and R.H. Schuster, *Characterisation of surface activity of carbon black and its relation to polymer-filler interaction.* Macromol. Mater. Eng., 2007: p. 885-916.

20. Suroso, W.S., D. Djoearsa, and M.S.M. Situmorang. *Carbon black manufacturing*. in *Indonesian Petroleum Association*. 1975.

21. Buchel, K.H., H.H. Moretto, and D. Werner, *Industrial inorganic chemistry*, ed. 2. 2008.

22. Gannon, R.E., et al., *Acetylene*, in *Kirk-Othmer Encyclopedia of Chemical Technology*. 2000, John Wiley & Sons, Inc.

23. Wang, R., K. Wu, and C. Wu, *Highly sensitive electrochemical sensor for toxic ractopamine based on the enhancement effect of acetylene black nanoparticles.* Analytical Methods, 2015. **7**(19): p. 8069-8077.

24. Neuss, G., *Chemistry for the IB diploma*. 2001: Oxford university press.

25. Krishnan, D., et al., *Energetic graphene oxide: challenges and opportunities.* Nano Today, 2012. **7**(2): p. 137-152.

26. Gilardi, R., D. Bonacchi, and M.E. Spahr, *Graphitic carbon powders for polymer applications*, in *Polymers and Polymeric Composites: A Reference Series*, S. Palsule, Editor. 2016, Springer Berlin Heidelberg: Berlin, Heidelberg. p. 1-25.

27. O'Dea, A.R., R.S.C. Smart, and A.R. Gerson, *Molecular modelling of the adsorption of aromatic and aromatic sulfonate molecules from aqueous solutions onto graphite.* Carbon, 1999. **37**(7): p. 1133-1142.

28. Pantea, D., et al., *Electrical conductivity of thermal carbon blacks: influence of surface chemistry.* Carbon, 2001. **39**(8): p. 1147-1158.

29. Medalia, A.I., *Electrical Conduction in Carbon Black Composites.* Rubber Chemistry and Technology, 1986. **59**(3): p. 432-454.

30. Balberg, I., *A comprehensive picture of the electrical phenomena in carbon black–polymer composites.* Carbon, 2002. **40**(2): p. 139-143.

31. Sánchez-González, J., et al., *Electrical conductivity of carbon blacks under compression.* Carbon, 2005. **43**(4): p. 741-747.

32. Li, Z.H., J. Zhang, and S.J. Chen, *Effects of carbon blacks with various structures on vulcanization and reinforcement of filled ethylene-propylene-diene rubber.* eXPRESS Polym. Lett., 2008. **2**: p. 10.

33. Ariu, G., *Influence of low – structure carbon black on the electrical, rheological and mechanical properties of graphite nanoplatelets/ethyl butyl acrylate composites*, in *Department of Materials and Manufacturing Technology*. 2013, CHALMERS UNIVERSITY OF TECHNOLOGY.

34. Donnet, J.-B. and E. Custodero, *Reinforcement of elastomers by particulate fillers*, in *The Science and Technology of Rubber (Fourth Edition)*. 2013, Academic Press: Boston. p. 383-416.

35. Larkin, P., *Introduction: Infrared and Raman Spectroscopy*, in *Infrared and Raman Spectroscopy*. 2011, Elsevier: Oxford. p. 1-5.

36. Nemanich, R.J., G. Lucovsky, and S.A. Solin, *Infrared active optical vibrations of graphite.* Solid State Commun., 1977. **23**(2): p. 117-120.

37. Ferrari, A.C. and D.M. Basko, *Raman spectroscopy as a versatile tool for studying the properties of graphene.* Nat Nano, 2013. **8**(4): p. 235-246.

38. Fultz, B. and J. Howe, *Diffraction and the x-ray powder diffractometer*, in *Transmission Electron Microscopy and Diffractometry of Materials*. 2008, Springer Berlin Heidelberg: Berlin, Heidelberg. p. 1-59.

39. Hu, Y.-H., et al., *Texture ZnO thin-films and their application as front electrode in solar cells.* SciRes., 2010. **2**.

40. Hu, C., et al., *Raman spectroscopy study of the transformation of the carbonaceous skeleton of a polymer-based nanoporous carbon along the thermal annealing pathway.* Carbon, 2015. **85**: p. 147-158.

41. Biscoe, J. and B.E. Warren, *An x-ray study of carbon black.* J. Appl. Phys., 1942. **13**(6): p. 364-371.

42. Ferrari, A.C. and J. Robertson, *Origin of the 1150-cm-1 Raman mode in nanocrystalline diamond.* Phys. Rev. B, 2001. **63**(12): p. 121405.

43. Jawhari, T., A. Roid, and J. Casado, *Raman spectroscopic characterization of some commercially available carbon black materials.* Carbon, 1995. **33**(11): p. 1561-1565.

44. Sadezky, A., et al., *Raman microspectroscopy of soot and related carbonaceous materials: spectral analysis and structural information.* Carbon, 2005. **43**(8): p. 1731-1742.

45. Ungár, T., et al., *Size and shape of crystallites and internal stresses in carbon blacks.* Compos. Part A-Appl. S., 2005. **36**(4): p. 431-436.

46. Tuinstra, F. and J.L. Koenig, *Raman spectrum of graphite.* J. Chem. Phys., 1970. **53**(3): p. 1126-1130.

47. Ferrari, A.C. and J. Robertson, *Resonant Raman spectroscopy of disordered, amorphous, and diamondlike carbon.* Phys. Rev. B, 2001. **64**(7): p. 075414.

48. Gruber, T., T.W. Zerda, and M. Gerspacher, *Raman studies of heat-treated carbon blacks.* Carbon, 1994. **32**(7): p. 1377-1382.

49. Ono, K., et al., *Influence of furnace temperature and residence time on configurations of carbon black.* Chem. Eng. J., 2012. **200–202**: p. 541-548.

50. Keller, J.U. and S. Reiner, *Adsorption Isotherms*, in *Gas Adsorption Equilibria: Experimental Methods and Adsorptive Isotherms*. 2005, Springer US: Boston, MA. p. 359-413.

51. Allen, T., *Particle size measurement*. 5 ed. Surface Area and Pore Size Determination. Vol. 2. 1997: Chapman & hall.

52. Lahaye, J. and G. Prado, *Formation of carbon particles from a gas phase: nucleation phenomenon.* Water, Air, Soil Pollut., 1974. **3**(4): p. 473-481.

53. German, R.M., *Handbook of mathematical relations in particulate materials processing*. 2008: wiley.

54. Munakata, H., *Development of nanoparticle composite technique for low Pt-loading PEFCs*, in *Nanoparticle technology handbook*, M.H. Makio Naito, Toyokazu Yokoyama, Kiyoshi Nogi, Editor. 2012, elsevier. p. 684.

55. Vidano, R.P., et al., *Observation of Raman band shifting with excitation wavelength for carbons and graphites.* Solid State Commun., 1981. **39**(2): p. 341-344.

56. Nakamizo, M., R. Kammereck, and P.L. Walker, *Laser raman studies on carbons.* Carbon, 1974. **12**(3): p. 259-267.

57. Socrates, G., *Infrared and Raman characteristic group frequencies: tables and charts*. 3 ed. 2001, England: John Wiley & Sons Ltd,. 366.

58. Chu, P.K. and L. Li, *Characterization of amorphous and nanocrystalline carbon films.* Mater. Chem. Phys., 2006. **96**(2–3): p. 253-277.

59. Wada, S. and A.T. Tokunaga, *Carbonaceous onion-like particles: a possible component of the interstellar medium*, in *Natural Fullerenes and Related Structures of Elemental Carbon*. 2006, Springer Netherlands: Dordrecht. p. 31-52.

60. Friedel, R.A. and G.L. Carlson, *Infrared spectra of ground graphite.* J. Phys. Chem., 1971. **75**(8): p. 1149-1151.

61. Kaneki, S., et al., *Organochemical characteristics of carbonaceous materials as indicators of heat recorded on an ancient plate-subduction fault.* Geochem. Geophys. Geosyst., 2016. **17**(7): p. 2855-2868.

62. O'Reilly, J.M. and R.A. Mosher, *Functional groups in carbon black by FTIR spectroscopy.* Carbon, 1983. **21**(1): p. 47-51.

63. Ono, K., et al., *Detailed kinetic analysis of the effect of benzene–acetylene composition on the configuration of carbon nanoparticles.* Chem. Eng. J., 2014. **250**: p. 66-75.

64. Considine, D.M. and G.D. Considine, *Carbon cycle (Nuclear)*, in *Van Nostrand's Scientific Encyclopedia*. 1995, Springer US. p. 540.

65. Tesner, P.A. and S.V. Shurupov, *Some physico-chemical parameters of soot formation during pyrolysis of methane and methane-acetylene and methane-benzene mixtures.* Symp. (Int.) Combust., 1994. **25**(1): p. 653-659.

66. Tesner, P.A. and S.V. Shurupov, *Some physico-chemieal parameters of soot formation during pyrolysis of hydrocarbons.* Combust. Sci. Technol., 1995. **105**(1-3): p. 147-161.

67. Wey, C., E.A. Powell, and J.I. Jagoda, *The Effect of Temperature on the sooting behavior of laminar diffusion flames.* Combust. Sci. Technol, 1984. **41**: p. 173.

APPENDIX

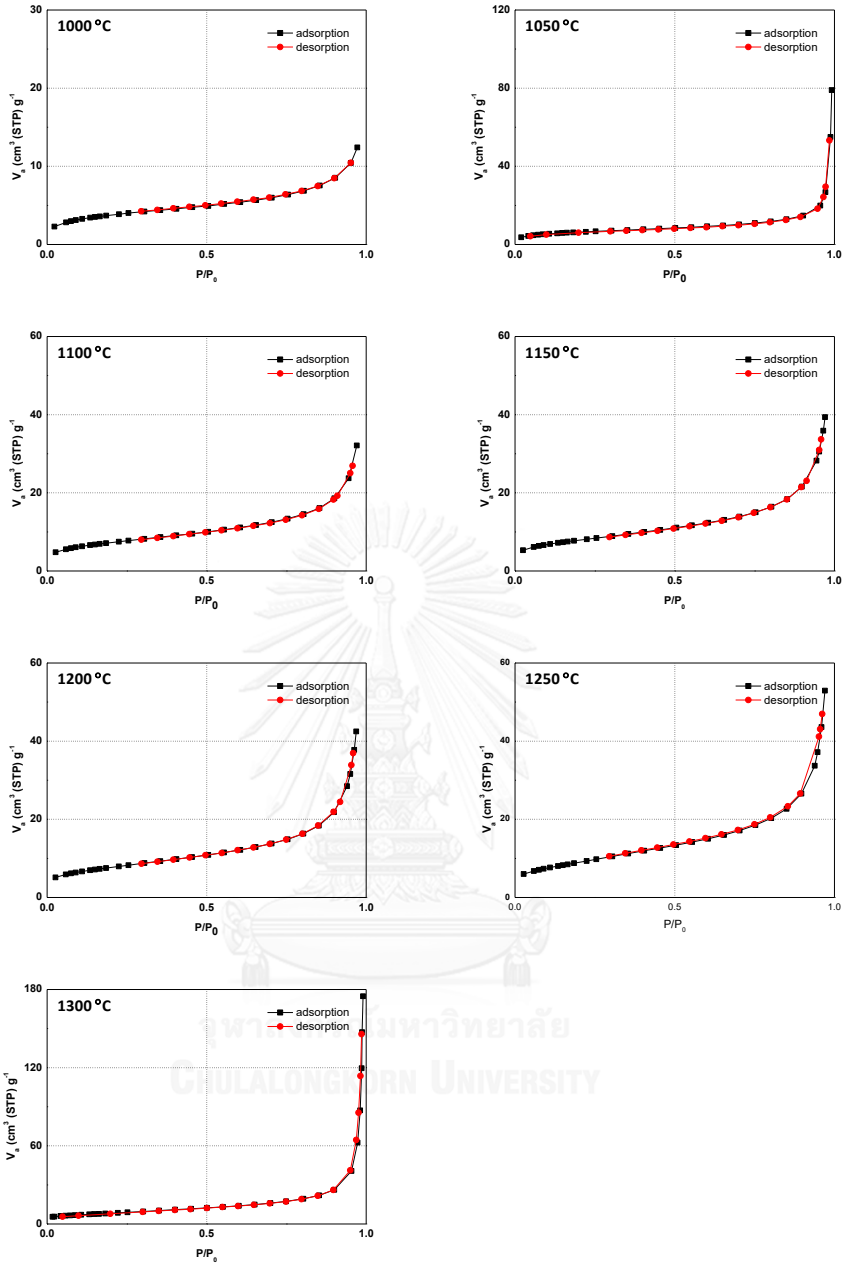

Fig. S1 Adsorption isotherm of acetylene black at different temperatures.

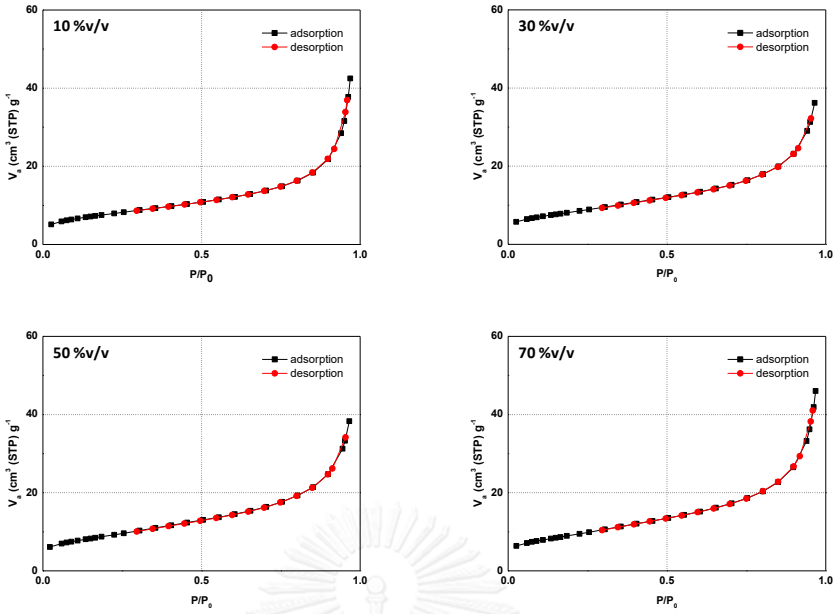

Fig. S2 Adsorption isotherm of acetylene black at different concentrations.

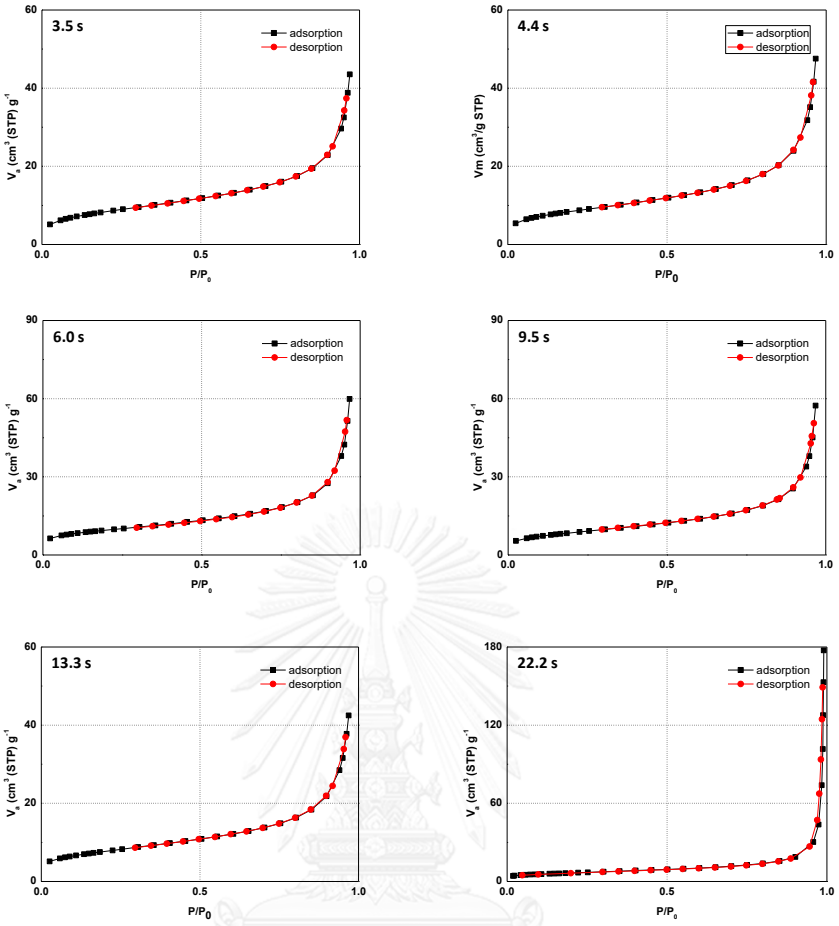

Fig. S3 Adsorption isotherm of acetylene black at different residence times.

VITA

Name: Miss Pimchanok Laowtaweerungruang

Birthday: 3 August 1992

Address: 99/134 Niranavenue Soi.Navamin51

Klongjan Bangkapi Bangkok 10240, Thailand

Email: wekyweky_6@hotmail.com

Education: B.Sc. in Chemistry (2014)

M.Sc. in Petrochemistry and Polymer Science (2017)

Chulalongkorn University, Bangkok, Thailand

Conference: Pure and Applied Chemistry International Conference 2016

Bangkok, Thailand

The 42nd Congress on Science and Technology of Thailand

The 3rd International Congress on Advanced Materials